Energy Conversion and Management 344 (2025) 120213

Contents lists available at ScienceDirect

Energy Conversion and Management

journal homepage: www.elsevier.com/locate/enconman

Research paper

Oxygen production via electrolysis: A model-based assessment of its impact on a climate-neutral German energy system

Luka Bornemann *, Jelto Lange, Martin Kaltschmitt

Institute of Environmental Technology and Energy Economics, Hamburg University of Technology, Eissendorfer Strasse 40, 21073 Hamburg, Germany

ARTICLE INFO

Dataset link: https://zenodo.org/records/15167498, Code and Data for Paper: Oxygen Production via Electrolysis: A Model-Based Assessment of Its Impact on a Climate-Neutral German Energy System (Original data)

Keywords:
Green hydrogen
Electrolysis
Oxygen
Energy system optimization

ABSTRACT

The integration of "green" hydrogen into the energy supply represents a key strategy for the defossilization of energy systems. However, its economic viability remains constrained by the currently high production costs. A possible strategy to enhance the economic feasibility of hydrogen-based energy systems is the system-integrated utilization of oxygen, a by-product of electrolysis. This study examines the potential of integrating electrolysis-derived oxygen into various industrial applications using an energy system optimization model of Germany. The analysis focuses on identifying the cost-saving potential, the resulting impact on the hydrogen and oxygen supply chains, and suitable industrial sites for oxygen utilization. The findings reveal that integrating electrolysis-derived oxygen into industrial processes offers substantial cost-saving opportunities while influencing the optimal configuration of hydrogen supply chains and infrastructure. Incorporating electrolysis-derived oxygen into existing industrial processes can reduce total system costs by up to 0.2% without significantly changing hydrogen infrastructure design or the average levelized costs of hydrogen. Further savings are achievable by introducing new applications such as oxy-fuel combustion and wastewater treatment. In this case, system costs can decrease by up to 1.3%, and average levelized costs of hydrogen can fall by 7%. These changes also shift optimal electrolyzer siting toward industrial locations with high oxygen demand. The high-value chemical industry, in particular, can cover nearly its entire newly created oxygen demand through electrolysis. The results highlight the systemic value of integrating electrolysis-derived oxygen and underscore the importance of including oxygen utilization in early hydrogen infrastructure planning.

1. Introduction

Hydrogen is increasingly recognized as a key element in the transition to renewable energy systems to mitigate climate change [1]. Beside its traditional use as an industrial feedstock, hydrogen is being explored for emerging applications such as seasonal energy storage and "green" fuel for selected segments of the transportation sector [2]. To comply with established greenhouse gas reduction targets, "green" hydrogen is produced using electrolyzers powered by electricity from renewable energy sources [3]. However, the current cost of "green" hydrogen production remains high [4], and reducing these costs is critical for enabling its large-scale deployment [5].

A promising strategy to enhance the economic feasibility of "green" hydrogen is the system-integrated utilization of oxygen, a by-product of electrolysis. By the year 2050, the global hydrogen demand is projected to range between 148 to 660 Mt/a [6]. If this demand is entirely met through water electrolysis, it would result in the production of 1184 to 5280 Mt/a of oxygen as a by-product. Currently, the global oxygen demand stands at approximately 500 Mt/a [7], with major consumption occurring in the iron and steel industry [8], the paper and pulp industry [9], the chemical industry [10], and in medical care [11]. Therefore, by the year 2050, oxygen generated as a by-product of hydrogen production via electrolysis could potentially exceed current global oxygen demand by up to a factor of ten.

Today, oxygen is mainly supplied via air separation processes (e.g., cryogenic separation [12], pressure swing adsorption, and membrane-based methods [13]) either as a main product or by-product. Typically, these methods are energy-intensive and costly [14]. Utilizing oxygen produced as a by-product of electrolysis can therefore help reduce energy consumption and costs associated with oxygen supply, while enhancing the economic viability of electrolyzers by generating additional revenue through the utilization or sale of the by-product oxygen [15].

Moreover, employing pure oxygen in sectors that have previously used it in limited quantities (e.g., glass industry [16], wastewater treatment [17], combustion air enrichment [14]), can improve process

* Corresponding author.
E-mail address: luka.bornemann@tuhh.de (L. Bornemann).

https://doi.org/10.1016/j.enconman.2025.120213
Received 11 April 2025; Received in revised form 6 June 2025; Accepted 11 July 2025
Available online 1 August 2025

Nomenclature

Sets

$\mathcal{C}$	Set of all components
$\mathcal{N}$	Set of all nodes
$\mathcal{T}$	Set of all time steps

Latin letters

c	Price [€/k Wh]
D	Specific mass demand [t/t_{prod}]
$\dot{E}$	Commodity flow [kW; kg/h]
E	Amount of commodity [kWh; kg]
M	Molar mass [g/mol]
n	Amount of substance [mol]
P	Electricity demand [kWh]
p	Specific electricity demand [kWh/kg]
q	Per capita wastewater production rate [L/(d pers)]

Greek letters

Δ	Difference [-]

Superscripts and Subscripts

air	Air
ASU	Air separation unit
avg	Average
bm	Biomass
c	Component
CH_4	Methane
D	Demand
d	Daily
EL	Electrolyzer
el	Electricity
n	Node
oxy	Oxy-fuel combustion
prod	Product
t	Time step
wwt	Wastewater treatment

Abbreviations

ASU	Air separation unit
BOD	Base oxygen demand
BOxD	Biochemical oxygen demand
CAPEX	Capital expenditures
CC	Carbon capture
EOD	Extended oxygen demand
H_2	Hydrogen
HVC	High-value chemicals
LCOE	Levelized costs of electricity
LCOH	Levelized costs of hydrogen
LCOO	Levelized costs of oxygen
LHV	Lower heating value
O_2	Oxygen
SOTE	Standard oxygen transfer efficiency
WWT	Wastewater treatment

efficiency and enhance carbon dioxide (CO_2) capture effectiveness, where applicable.

Previous research mainly explored the integration of electrolyzers to replace fossil fuels with hydrogen in applications that already utilize oxygen. One study highlighted the viability of producing oxygen on-site via electrolysis in healthcare facilities, where hydrogen is simultaneously used for internal energy needs. For oxygen market prices above 3 to 4 €/kg, on-site production via an electrolyzer is more cost-effective than external procurement [11]. Another investigation demonstrated that surplus electricity can be effectively utilized in pulp mills by generating hydrogen for heat production and employing oxygen in existing chemical processes [9]. Under specific conditions, producing oxygen via electrolysis and selling the hydrogen has also been shown to be more advantageous than purchasing oxygen from external sources [10]. In the wastewater treatment sector, a circular system was proposed in which hydrogen produced by a nearby electrolyzer is used for biological methanation, while oxygen is utilized for the treatment process, resulting in both energy savings and emissions reductions of up to 40% [18]. Nhuchhen et al. [19] present a concept in which oxy-fuel combustion is combined with carbon capture and storage to enhance the energy efficiency and to achieve climate neutrality of cement clinker production. The study shows that utilizing the by-product oxygen from electrolysis is more cost-effective than oxygen produced via air separation units (ASUs), enabling electrolyzer operators to generate additional revenue of approximately 0.3 USD/kg through oxygen sales. Another study proposes a waste heat utilization concept for a cement plant, in which an organic Rankine cycle is used to generate electricity for operating an electrolyzer. The hydrogen and oxygen produced are then utilized together with methane in an oxy-fuel process within a rotary kiln. By substituting oxygen from ASUs and reducing the methane required for combustion, the plant's overall energy demand can be significantly lowered [20].

Despite these promising findings, the broader impact of electrolyzer-derived oxygen utilization across various sectors and the overall energy system remains insufficiently understood. While these studies highlight the economic benefits of combined hydrogen and oxygen use, they often fail to compare these approaches with alternative, potentially more cost-effective defossilization technologies. In addition, most of them emphasize decentralized on-site electrolysis and air separation, overlooking the potential cost advantages of centralized, large-scale deployment, which may be more attractive to operators. It also remains unclear how much electrolysis-derived oxygen will be available in the future, and where and when it will be produced. To overcome these limitations, a system-wide approach is needed to assess whether it is more beneficial to site electrolyzers for optimal oxygen utilization, or to prioritize cost-effective hydrogen production, leaving oxygen supply to conventional air separation methods.

To close this research gap, this paper employs an energy system optimization model focused on Germany to assess the potential for utilizing oxygen produced from electrolyzers as by-product. From a cost-optimal perspective, this study evaluates the extent to which electrolyzer-generated oxygen can be integrated into existing supply chains, the resulting cost savings, and the corresponding impacts on both the hydrogen and oxygen supply chains. Based on this investigation, this study identifies the most promising locations and industrial applications that could benefit from the use of electrolysis-derived oxygen.

The paper is structured as follows. Section 2 outlines the methodological approach, detailing the energy system model, the model extensions, and the assessment criteria. Section 3 introduces the case studies and scenarios analyzed, followed by the presentation and discussion of the results in Sections 4 and 5, respectively. Lastly, Section 6 concludes the overall study.

2. Methodological approach

The methodological approach to answer the research question outlined above is depicted in Fig. 1, featuring a model-based design and operational optimization of the German energy system. Two case

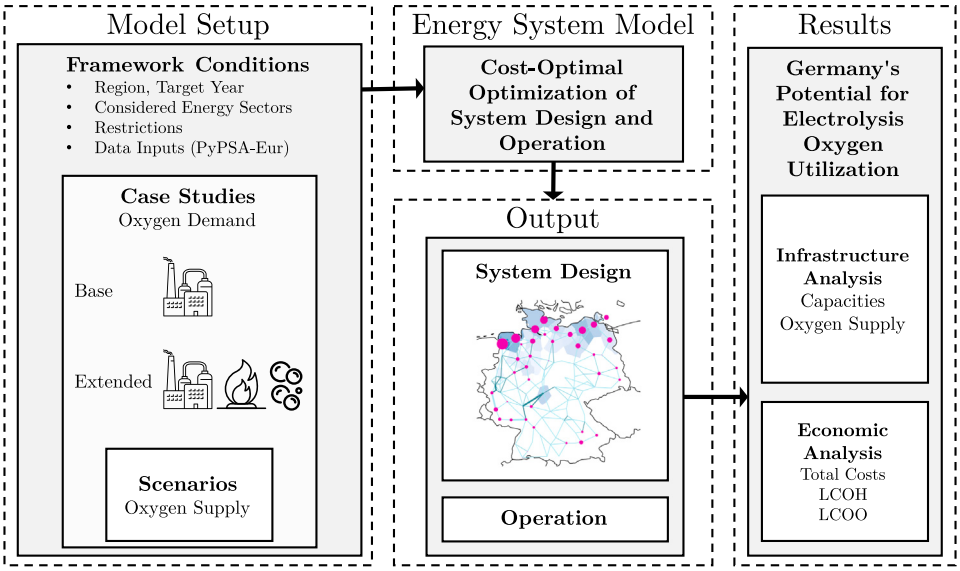

Fig. 1. Methodological approach (LCOH: Levelized cost of hydrogen, LCOO: Levelized cost of oxygen).
Source: Adapted from [2].

studies are established, differentiated by their consideration of possible oxygen applications and the corresponding oxygen demands. For each case study, scenarios defining oxygen supply and utilization boundaries are developed. These case studies and scenarios — combined with overarching framework conditions and system assumptions — are evaluated through an optimization model to assess Germany's overall potential for utilizing oxygen provided as a by-product from electrolyzers. In addition to optimizing the entire energy supply (i.e., the energy system design and operation), the model places particular emphasis on the expansion and operation of the oxygen and hydrogen supply infrastructure, enabling a comprehensive infrastructure and economic assessment of electrolysis oxygen integration.

2.1. Energy system model

The studies in this paper are conducted using PyPSA-Eur [21], an open-source capacity expansion model of the European energy system. The fundamental structure and functionality of the model are outlined below.

The model optimizes system design and operation of the European energy system by jointly optimizing the investment and operation of generation, storage, conversion, and transmission infrastructure. It employs a linear optimization framework to minimize total annual system costs while accounting for constraints such as transmission capacities, energy demands, and carbon emission limits.

The model integrates energy demands across different sectors — including electricity, transport, heating, and industry — using open data sources as inputs. It simulates intra-European energy flows, assuming unlimited fossil fuel imports but excluding cross-border energy exchange beyond Europe. The model represents system interconnections by capturing the spatial and temporal distribution of energy demand and renewable energy supply potential across the continent. Spatially, energy demand, renewable energy supply potential, and infrastructure data are allocated to so-called regional nodes, while temporally, the model supports a minimum granularity of 1 h.

For modeling the hydrogen infrastructure, hydrogen demand is considered both for direct use as a raw material (e.g., in the steel industry) and as a feedstock in the chemical sector (e.g., for ammonia, synthetic methane, and liquid hydrocarbons). In addition to these partially existing hydrogen markets, potential future applications of hydrogen and its derivatives are also taken into account, including use in the transport sector (e.g., heavy-duty vehicles, aviation, and shipping) as well as for electricity generation in gas turbines and fuel cells.

Hydrogen production pathways modeled include electrolysis and methane reforming with carbon capture and storage (CCS). Storage is realized in underground salt caverns, and hydrogen transport is represented through pipeline systems, either retrofitted natural gas pipelines or newly constructed hydrogen pipelines. A brief overview of the mathematical formulation of the model and its optimization is outlined in Appendix A.

Model extensions. PyPSA-Eur does not originally include oxygen as a commodity. Therefore, oxygen is integrated as a carrier along with the necessary infrastructure into the model (Fig. 2). Oxygen demand is defined for various possible industrial applications (as defined in Section 3.2). The model allows for meeting this demand either through the construction of ASUs or by utilizing oxygen produced as a by-product of electrolysis.

In addition to oxygen, ASUs produce also other industrial gases that can serve as feedstocks, such as argon. To account for this coupled production in system planning, a demand for industrial argon is explicitly included. This demand can only be satisfied by ASUs, implying that even with large-scale integration of electrolysis-derived oxygen, a minimum share of ASUs must remain operational to meet the required argon demand (as defined in Section 3.2). For simplicity, the argon demand is modeled as an aggregated total across the entire energy system, rather than being spatially distributed. Moreover, the argon demand is considered inelastic and cannot be substituted by other industrial gases.

Excess oxygen, whether produced by ASUs or electrolyzers, can either be stored in oxygen storage facilities or released into the atmosphere. Similarly, any surplus argon—co-produced with oxygen in ASUs—may also be stored in argon storage facilities or vented, as needed. This reflects the modeling assumption that ASUs generate oxygen and argon in fixed mass proportions, meaning that for each unit of oxygen produced, a corresponding fraction of argon is simultaneously generated. Given that electrolysis-derived oxygen is primarily intended for local use, it is assumed that oxygen transport is limited to short distances. As a result, distribution is allowed within a node but not between neighboring nodes. Table B.1 summarizes the techno-economic parameters of the components described above.

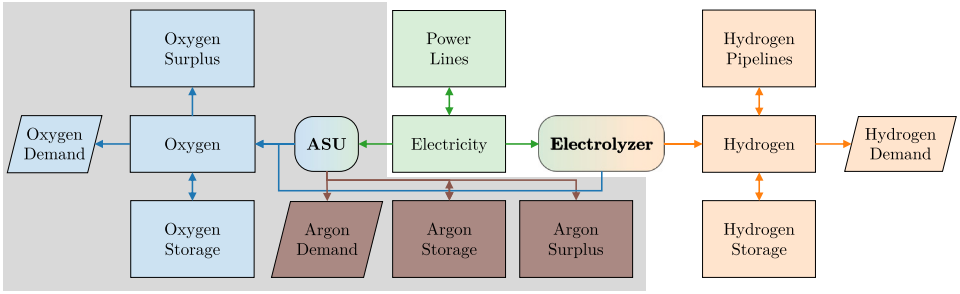

Fig. 2. Overview of the oxygen model extension marked in gray (ASU: Air Separation Unit).
Source: adapted from [2]

2.2. Assessment criteria

The analysis of the potential for utilizing electrolysis-derived oxygen is conducted through both infrastructure and economic evaluations.

The infrastructure evaluation considers the following parameters:

- Local and total installed capacities of ASUs and electrolyzers.
- Quantities of oxygen produced by these capacities and the proportion of electrolyzer-generated oxygen that can be integrated into the existing and possible future demand pattern. Since ASUs constitute the established oxygen infrastructure, the integration framework assumes that, at each node ($\forall n \in \mathcal{N}$), locally produced oxygen from ASUs is utilized first, with any remaining demand covered by electrolyzer-produced oxygen.

The economic evaluation focuses on the following parameters:

- Total costs (i.e., investment and operational expenses) of the modeled energy system, which includes not only the costs related to oxygen supply but also the overall costs of each other sector (e.g., electricity generation, transportation, industrial sectors) modeled within the system.
- The levelized cost of oxygen (LCOO) and the levelized cost of hydrogen (LCOH).

The LCOO and LCOH are calculated using Eqs. (1) and (2), respectively. For the LCOO, the annualized capital expenditures $CAPEX_{n,c}$ of the oxygen-related components ($\forall c \in C^{O_2}$) and the electricity costs for oxygen production via the ASU are divided by the total oxygen demand $E^{D}_{O_2}$. The electricity costs are determined by multiplying the local electricity marginal price $c_{n,t,el}$ at each time step ($\forall t \in \mathcal{T}$) by the local electricity consumption of the ASU $\dot{E}^{ASU}_{n,t,el}$. This is then summed across all time steps, adjusted by the time step length Δt, with the balance calculated for each node ($\forall n \in \mathcal{N}$), before being summarized to derive the total oxygen costs.

$$LCOO = \frac{1}{E^{D}_{O_2}} \sum_{n \in \mathcal{N}} \left(\sum_{c \in C^{O_2}} CAPEX_{n,c} + \Delta t \sum_{t \in \mathcal{T}} c_{n,t,el} \dot{E}^{ASU}_{n,t,el} \right) \tag{1}$$

Similarly, the LCOH are calculated for all hydrogen-related components ($\forall c \in C^{H_2}$). However, in this case, the revenue from oxygen sales is also considered. This revenue is the product of the local oxygen marginal price c_{n,t,O_2} and the locally integrated electrolysis oxygen $\dot{E}^{EL}_{n,t,O_2}$.

$$LCOH = \frac{1}{E^{D}_{H_2}} \sum_{n \in \mathcal{N}} \left(\sum_{c \in C^{H_2}} CAPEX_{n,c} + \Delta t \sum_{t \in \mathcal{T}} \left(c_{n,t,el} \dot{E}^{EL}_{n,t,el} - c_{n,t,O_2} \dot{E}^{EL}_{n,t,O_2} \right) \right) \tag{2}$$

3. Model setup

The following sections outline the system assumptions applied in the energy system model and describe the case studies and scenarios developed for this analysis. The system assumptions apply identically to all scenarios and case studies.

3.1. System assumptions and framework conditions

This study focuses solely on Germany allowing for a detailed analysis of industrial oxygen supply while managing the computational complexity. The reference year is set to 2045, aligned with Germany's climate neutrality goal [22]. Accordingly, no CO_2 emissions may be present in the system-wide balance. However, local CO_2 emissions are permitted if they are offset through direct air capture systems and/or carbon capture and storage. Carbon capture and storage is limited to 100 Mt/a, with associated storage costs of 10 €/t [21]. Techno-economic parameters are designed to reflect anticipated technological advancements by that year, while industrial energy demands are aligned with future defossilization pathways (e.g., steel production through direct reduction of iron).

To accurately represent the expected availability of electrolyzer-derived oxygen based on realistic hydrogen production levels, the study accounts for all hydrogen-related sectors (i.e., electricity, transport, industry). Hydrogen production is limited to electrolysis only.

- In the electricity sector, hydrogen is incorporated through its production using electrolyzers and its subsequent reconversion into electricity (e.g., through gas turbines and fuel cells).
- For the transportation sector, hydrogen demand is restricted to liquid hydrocarbon applications in shipping and aviation, with land-based transport assumed to be fully electrified.
- In industrial applications, hydrogen demand arises both directly (e.g., steel production) and indirectly (e.g., synthetic methane synthesis). Additionally, the industrial sector includes a representative oxygen demand from German industry (as defined in Section 3.2).

For spatial resolution, 90 nodes are selected, distributed across Germany. Temporally, the time series data for 2045 is aggregated into 3-hour intervals to limit computational effort while maintaining sufficient resolution for renewable energy availability. The standard weather data in PyPSA-Eur is used [23], based on 2013 SARAH-2 [24] and ERA-5 [25] datasets for renewable energy resource modeling.

3.2. Case study definition

Two case studies are investigated, differing in the considered applications of oxygen. Their characteristics and assumptions are outlined below.

Table 1
Overview of the specific oxygen demands and total argon demand used in the Base Oxygen Demand case study.

Industry	Unit	Value	Ref.
Integrated Steelworks	t_{O_2}/t_{prod}	0.135742	[8,28]
Electric Arc Furnaces	t_{O_2}/t_{prod}	0.0536	[29]
Direct Reduced Iron	t_{O_2}/t_{prod}	0.05293	[30]
Ethylene Oxide	t_{O_2}/t_{prod}	0.363[a]	own calc., [31]
Hydrogen Peroxide	t_{O_2}/t_{prod}	0.941[a]	own calc., [31]
Sulfuric Acid	t_{O_2}/t_{prod}	0.327[a]	own calc., [31]
Pulp Production	t_{O_2}/t_{prod}	0.02	[9]
Medical Use	$t_{O_2}/(a\,pers)$	0.0011122	[32]
Other Industrial Sectors	t_{O_2}/t_{prod}	0.024[b]	own calc.
Argon	Mt_{Ar}/a	0.3	[33]

[a] Based on stoichiometric reaction ratios.

[b] The value was determined to ensure that, along with other specific demands defined in the model, it results in a total oxygen demand of 9 Mt/a, which corresponds to the German oxygen production in 2017 [34], based on today's industrial production specified in the model.

3.2.1. Case 1: Base Oxygen Demand

The *Base Oxygen Demand* (BOD) case study focuses on industrial applications that currently utilize pure oxygen (i.e., steel production, pulp production, glass production, non-ferrous metal production, medical uses). Oxygen is also employed in producing basic chemicals such as ethylene oxide, hydrogen peroxide, and sulfuric acid, alongside smaller applications in food packaging, metal processing, and electronics.

In the energy system model, each application is assigned a mass-specific oxygen demand per manufactured product within the respective industrial sector.

- For steel production, distinctions are made between the integrated steelworks route, the electric arc furnace route, and direct iron reduction processes.
- Regarding the glass and non-ferrous metal production, a complete electrification of these industries by the year 2045 is assumed [26], resulting in no modeled oxygen demand despite the fact that these sectors currently utilize oxygen in their processes.
- Since the aforementioned basic chemicals are not explicitly represented within the defined model sectors, they are categorized under the basic chemicals sector.
- All other small-scale oxygen applications are allocated to the 'other industrial' sectors.
- The oxygen demand for medical use is distributed according to the local population density. As electrolysis-derived oxygen can fulfill medical-grade standards without additional purification [27], its use in the medical sector is permitted within the model.

To determine the specific oxygen demand of the considered applications, it is assumed that the current specific oxygen input remains unchanged in the future. Table 1 provides a summary of the specific oxygen demands for each industry application as well as the total argon demand considered here.

3.2.2. Case 2: Extended oxygen demand

As hydrogen production from electrolyzers is expected to generate a significant surplus of oxygen in the future, a further case study explores the potential utilization of this excess. One application is the transformation of existing industrial combustion processes to oxy-fuel combustion, where fuels are burned with pure oxygen instead of air. This method can enhance fuel efficiency [35] and facilitates more effective carbon capture [19].

Within the model, oxy-fuel combustion is allowed for implementation in industrial applications, containing sub processes that are expected to continue to rely on combustion processes to cover their process heat demand by the year 2045 (i.e., steel [21], high-value chemicals (HVC) [21,26,36], cement [21], alumina [21]). Based on the temperature requirements of the heat needed [37], methane (either from fossil origins or from biogenic and synthetic sources) combustion is pre-specified for these industries [21]. The ratio between synthetic and fossil-based methane in the respective industry emerges endogenously from the optimization (i.e., is a degree of freedom within the optimization). Accordingly, local CO_2 emissions are permitted if they are offset through direct air capture systems and/or carbon capture and storage (see Section 3.1). It is assumed, that the fuel demand can be reduced by 20% through oxy-fuel combustion compared to traditional air-fueled combustion [35]. The calculation of the specific oxygen demand for oxy-fuel combustion is defined in Eq. (B.1).

Furthermore, pure oxygen can be utilized in wastewater treatment plants to decrease the energy consumption per capita of the air blowers from 56 to 11 kWh/(a pers) [17]. The derivation of the needed oxygen and the resulting electricity consumption can be found in Eq. (B.2) and (B.3). The oxygen and electricity demand for wastewater treatment are distributed according to the local population density.

These two additional oxygen applications are implemented as expansion options in this case study in addition to the existing oxygen demand from the BOD case study (Table 1), allowing the resulting extended oxygen demand to emerge endogenously from a cost-optimized energy supply. The integration of oxy-fuel combustion and wastewater treatment into the existing model and their techno-economic parameters are depicted in Fig. 3 and Table B.3, respectively.

3.3. Scenario definition

Each of the two case studies is analyzed based on four scenarios. These scenarios establish boundary conditions for oxygen supply within the optimization. In every scenario, the operational strategies for both ASUs and electrolyzers are subject to optimization. Additionally, the scenarios vary based on whether infrastructure capacities are optimized and whether the utilization of oxygen generated through electrolysis is allowed. The scenarios are partially interdependent, as certain results from preceding scenarios serve as starting points for subsequent ones. Fig. 4 illustrates these interrelations, along with the respective constraints and degrees of freedom concerning the design of the oxygen and electrolyzer infrastructure within each optimization. These aspects are explained in more detail below.

- **Reference Scenario (S1).** The S1-scenario reflects the status quo, in which hydrogen and oxygen supply systems are planned independently. In this setup, the model separately optimizes the capacity and operation of ASUs and electrolyzers to meet local demands for hydrogen, oxygen, and argon—without considering the use of oxygen produced as a by-product of electrolysis. Since the real ASU infrastructure is not explicitly modeled, this scenario adopts a greenfield approach. A distinction between the two case studies arises only from differences in local oxygen demand: while the BOD case study includes only baseline applications, the EOD case study additionally incorporates extended uses, potentially leading to varying demand levels. This variation is not predefined but emerges as an endogenous outcome of the optimization process. If no extended applications — requiring exclusive supply from ASU-produced oxygen — are included, the S1-scenario remains identical across both case studies. In addition, scenario S1 serves as the starting point for scenarios S2 and S3. One outcome of the optimization in scenario S1 is the determination of optimal local electrolyzer and ASU capacities. These optimal ASU capacities are carried over to scenarios S2 and S3, while the electrolyzer capacities from scenario S2 are reused in scenario S3 (see Fig. 4).

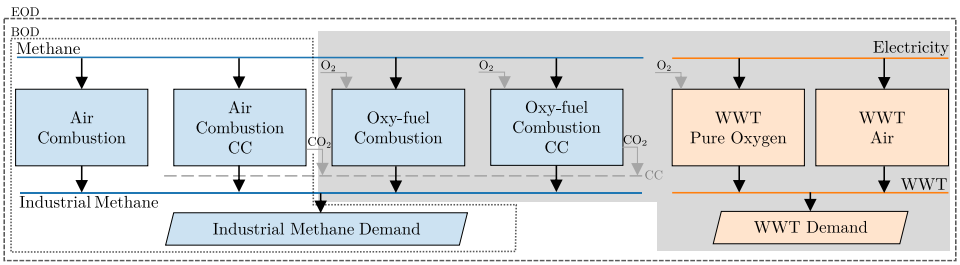

Fig. 3. Overview of the extended oxygen usage model extension marked in gray. In addition, the system boundaries of the Base Oxygen Demand (BOD) and Extended Oxygen Demand (EOD) case studies are shown (CC: Carbon Capture, WWT: Wastewater Treatment).

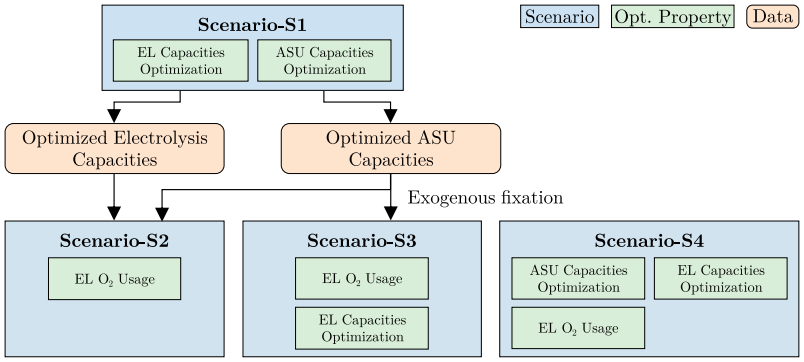

Fig. 4. Flowchart of the considered scenarios and their interconnections. The property "EL O_2 Usage" indicates that the utilization of electrolysis-derived oxygen is allowed as part of the optimization of the oxygen supply. (ASU: Air Separation Unit, EL: Electrolysis, Opt: Optimization).

- **Optimizing the Utilization of Electrolysis Oxygen Without Consideration in the Design Stage (S2).** The S2-scenario illustrates a situation where the oxygen produced through electrolysis can be used additionally, or as a 'bonus', without having been considered in the initial design of the hydrogen supply. In this context, the capacities for ASUs and electrolyzers are fixed exogenously based on the outcomes of the scenario S1 and are therefore not treated as degrees of freedom within the optimization (see Fig. 4). The model now allows for the utilization of electrolysis oxygen within the optimization process. However, since the infrastructure capacities remain fixed, the optimization focuses exclusively on the operational aspects of both the ASUs and the electrolyzers.
- **Optimizing the Hydrogen Supply Infrastructure Incorporating the Utilization of Electrolysis Oxygen in Parallel to the Existing Oxygen Infrastructure (S3).** The S3-scenario represents a situation where, alongside the existing oxygen supply infrastructure, the potential use of oxygen from electrolysis is considered in designing the hydrogen supply infrastructure. In the energy system model, the capacities of the ASUs remain fixed, based on the results from the S1-scenario. However, the electrolyzer capacities can now be freely optimized while incorporating the utilization of electrolysis oxygen.
- **Simultaneous Design Optimization of the Oxygen and Hydrogen Supply Infrastructure Including the Utilization of Electrolysis Oxygen (S4).** In the S4-scenario, the optimization is conducted from a greenfield perspective, allowing for the simultaneous design of both the oxygen and hydrogen supply infrastructures. This comprehensive approach aims to evaluate the full potential of integrating electrolysis-derived oxygen. In contrast to the S1-scenario, the optimization here explicitly incorporates the possible utilization of oxygen produced via electrolysis.

The scenario descriptions focus solely on the differences in the optimization of oxygen and hydrogen supply. In each scenario, the design and operation of the remaining energy system (i.e., electricity, transport, industrial sectors; see Section 3.1) are also optimized.

4. Results

The results are presented in the following sections. The analysis comprises both infrastructure (Section 4.1) and economic evaluations (Section 4.2). The infrastructure analysis focuses on the installed capacities of ASUs and electrolyzers, as well as the amount of oxygen they produce. Building on these findings, the economic analysis evaluates the potential cost savings resulting from the integration of electrolysis oxygen into the energy system.

4.1. Infrastructure assessment

The infrastructure assessment first examines the installed capacities of ASUs and electrolyzers at both national (Section 4.1.1) and local levels (Section 4.1.2), along with the total quantities of oxygen produced. Subsequently, industries that could particularly benefit from the provision of oxygen generated by electrolyzers are identified in Section 4.1.3.

4.1.1. Overall capacity and production assessment

Fig. 5 displays the total installed capacities of ASUs and electrolyzers, as well as the quantities of oxygen produced.

Base Oxygen Demand. In the S1-scenario, the ASU capacity is designed to exactly meet the given oxygen demand. This capacity remains unchanged in the S2- and S3-scenarios (as defined in Section 3.2). In these two scenarios, the integration of electrolysis-derived oxygen reduces the amount of oxygen produced by ASUs to a level that still satisfies the argon demand, given that argon is a by-product of ASU-based oxygen production. Any additional oxygen demand that exceeds the amount generated as a by-product of argon production is supplied by electrolysis. In the S4-scenario, the installed ASU capacity is specifically dimensioned to avoid oversizing, with ASUs operating at full capacity primarily to fulfill the argon demand—making oxygen a by-product in this case.

Regarding electrolyzers, in all scenarios, the amount of electrolysis-produced oxygen exceeds the demand; i.e., a significant portion of the

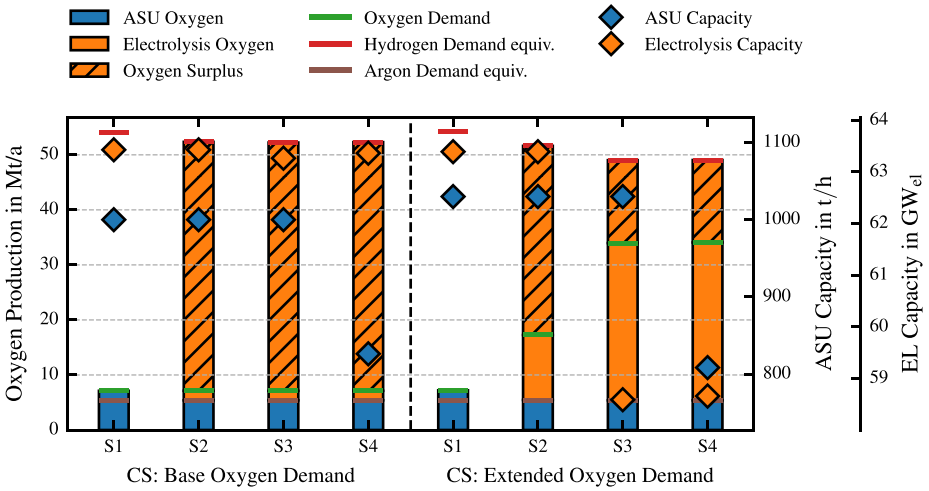

Fig. 5. Total installed capacities of the air separation unit (ASU) and electrolysis (EL), along with the resulting oxygen production volumes across all scenarios for both case studies (CS). Additionally, the industrial demands for oxygen, hydrogen, and argon (converted to an equivalent amount of oxygen) are highlighted, as well as surplus oxygen from electrolysis. For comparability, the equivalent hydrogen demand is offset by the ASU oxygen production to align with electrolyzer-derived oxygen production.

electrolysis oxygen cannot be utilized within the given markets. Across all scenarios, the electrolyzer capacity remains nearly unchanged, and the amount of oxygen produced is directly tied to the hydrogen demand. Consequently, the consideration of electrolysis-derived oxygen utilization does not influence the design (i.e., total capacity) or operation (i.e., total hydrogen amount) of the electrolyzers at the national level in any of the scenarios.

Extended Oxygen Demand. Regarding the ASUs, a similar trend is observed in the S1-scenario. The capacity and quantities of oxygen produced are slightly higher than those in the BOD case study, with only a small additional amount of oxygen being produced for wastewater treatment purposes (see Fig. 9). The findings from the BOD case study apply equally to the other scenarios of the EOD case study. The additional oxygen applications do not justify the extended use of oxygen derived from ASUs.

In contrast, the results for electrolyzers show a distinct pattern. Starting in scenario S2, additional electrolytic oxygen is integrated by incorporating further oxygen applications — such as oxy-fuel combustion and wastewater treatment — significantly surpassing the utilization observed in the BOD case study. The trend expands in scenario S3, with nearly all industrial combustion processes transitioning to oxy-fuel combustion (see Fig. 9). These changes result in significant methane savings, allowing the conserved methane to be redirected to other applications. This, in turn, reduces the system-wide total hydrogen demand and causes the total electrolyzer capacity to decrease from ca. 63 GW_{el} to around 59 GW_{el}. Consequently, the production of both hydrogen and oxygen declines. By scenario S4, no further changes are observed at the national level compared to scenario S3.

4.1.2. Capacity assessment at local level

Fig. 6 shows the installed ASU and electrolyzer capacities at each location for the S1- and S4-scenario of both case studies. These scenarios have been selected in order to depict all key trends as compactly as possible. The results for the S2- and S3-scenarios can be found in the appendix in Figs. C.1–C.7.

Base Oxygen Demand. As explained in Section 4.1.1, the total installed ASU capacity decreases from S1 to S4. Regarding scenario S4, this leads to a slightly more even distribution. Beyond this, however, the integration of electrolysis-derived oxygen has no significant impact on the ASU value chain (see also Figs. C.5 and C.7).

A similar observation applies to the siting and design of the electrolyzers. While isolated changes to local capacities occur (see also Figs. C.2 and C.7), these variations are negligible overall, as the total distribution and capacity remain nearly unchanged.

Extended Oxygen Demand. Significant differences arise between the S1- and S4-scenario due to potential additional oxygen applications. Regarding ASUs, scenario S1 exhibits a pattern similar to that of the BOD case study, whereas the distribution shifts significantly in scenario S4. Although the total installed capacity is of a comparable magnitude to scenario S4 in the BOD case study, local capacities are distributed less evenly. At many locations, the capacity is reduced, while a few sites still require high capacities (see also Figs. C.6 and C.7).

This behavior results from the siting of the electrolyzers. The integration of additional oxygen applications, supplied by electrolysis-derived oxygen, introduces an economic incentive to distribute electrolyzers more evenly across locations, resulting in the installation of smaller, more decentralized located electrolyzers. This decentralized production of hydrogen and oxygen enables the substitution of some local ASU capacities and the oxygen they generate by electrolysis-derived oxygen. This is visualized on the map of Germany in Fig. 7. In the S1-scenario (without electrolysis oxygen utilization), large electrolyzers are primarily installed in Northern Germany. This siting strategy leverages the region's low electricity costs, primarily resulting from high availability of offshore wind power. In contrast, in the S4-scenario, electrolyzers are located more prominently at industrial sites (for reference see Fig. C.8) to maximize oxygen integration. The focus shifts from producing hydrogen at the lowest possible cost to minimizing overall system costs by leveraging synergies between hydrogen and oxygen production.

4.1.3. Industrial oxygen supply assessment

Fig. 8 illustrates the oxygen demand and supply across various industrial sectors for all scenarios in the two case studies. The oxygen supply is further divided into contributions from ASUs and electrolysis-derived oxygen. For calculating these proportions, it is assumed that locally produced oxygen from the ASU is first used to meet the process-related oxygen demand (BOD). Any potential excess oxygen from the ASUs is allocated to the extended oxygen demand applications (EOD). The remaining demand, both BOD and EOD, is fulfilled using electrolysis-derived oxygen.

Base Oxygen Demand. In the scenario, where electrolysis oxygen is used but not explicitly included in the system design (S2), 18% (steel production) to 34% (pulp production) of the oxygen demand is covered by electrolysis-derived oxygen. In scenarios S3 and S4, these shares shift slightly due to isolated local changes in electrolysis capacities (see Figs. 6 and C.7). On average, this results in a supply share of ca. 24% across all industries, consistent with the findings in Section 4.1.1, with no industry standing out significantly in relative terms.

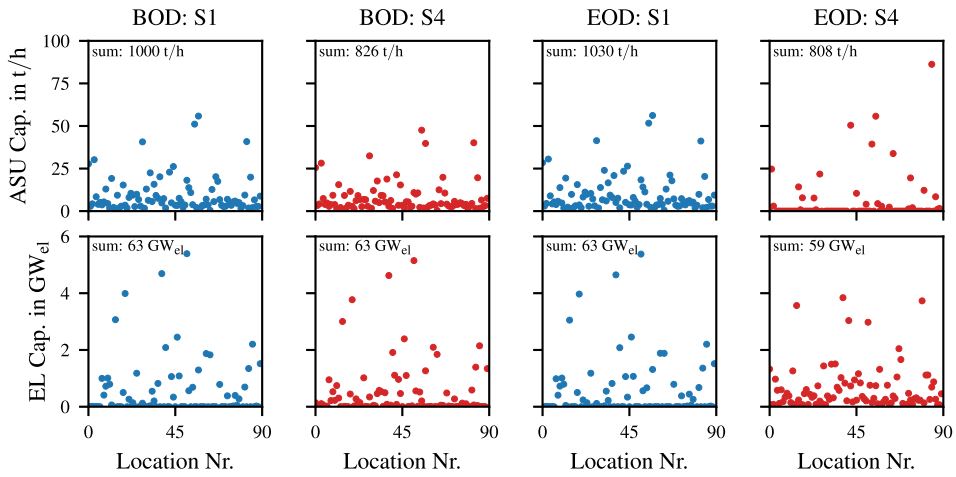

Fig. 6. Installed capacity of the air separation unit (ASU) and electrolysis (EL) in each node under consideration of scenarios S1 and S4 for both case studies (BOD: Base Oxygen Demand, EOD: Extended Oxygen Demand).

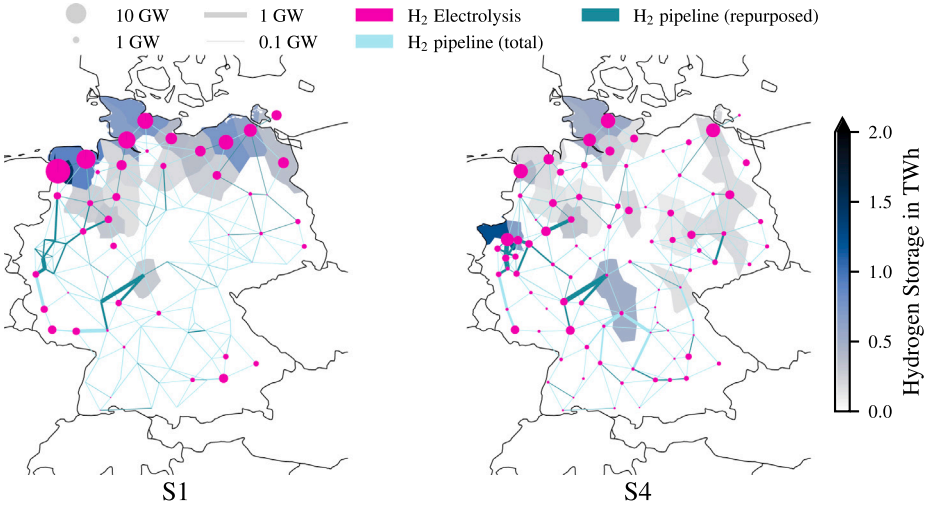

Fig. 7. Map of Germany of the 'Extended Oxygen Demand' case study for the scenarios S1 and S4. The local electrolysis and hydrogen storage capacities as well as the expansion of the hydrogen network pipelines are shown.

In absolute terms, steel production and smaller-scale applications (summarized under other industries) benefit the most from the supply of electrolysis-derived oxygen. Oxygen utilization from electrolysis in the steel industry is particularly advantageous, as this industrial application requires both hydrogen and oxygen through the direct reduced iron process route. As a result, local hydrogen and oxygen production via electrolyzers creates notable synergies.

Extended Oxygen Demand. The consideration of oxy-fuel and wastewater treatment applications leads to a more decentralized distribution of electrolyzer locations (see Section 4.1.2). For the BOD applications (i.e., pulp, basic chemicals, other industries, medical) in scenarios S2 and S3, no significant changes occur compared to the BOD case study. However, in scenario S4, where the ASU distribution is also adjusted (see Section 4.1.2), the supply share of electrolysis oxygen increases to as much as 77%.

For the EOD applications (i.e., steel, high-value chemicals, cement, alumina, wastewater treatment), several effects are observed. In the S1-scenario, no oxy-fuel processes are implemented, and only a small fraction of wastewater treatment processes are converted, relying solely on oxygen from ASUs, as shown in Fig. 9. Significant development of these extended oxygen applications occurs only with the integration of electrolysis-derived oxygen (S2), which fully supplies these processes. When the utilization of electrolysis-derived oxygen is incorporated into hydrogen infrastructure planning (S3 and S4), the share of extended oxygen applications increases further. Most industrial combustion processes are converted to oxy-fuel processes, and ca. 60% of wastewater treatment processes convert to a pure oxygen supply (see Fig. 9).

The S4-scenario is notable because, for the first time, non-negligible quantities of oxygen from ASUs are also utilized for these applications (Fig. 8). Since the total amount of oxygen produced by the ASUs remains identical between scenario S3 and scenario S4 (see Section 4.1), the difference in ASU-oxygen utilization is attributed to a shift in the ASU production sites (see Figs. C.6 and C.7). The ASUs are now operated primarily to meet argon demand, which is location-independent. As a result, the selection of ASU sites is more flexible, leading to a more even distribution of absolute production volumes across various types of oxygen demand. This approach helps balance potential fluctuations in oxygen supply from electrolyzers.

These overall findings suggest that industries with combustion processes (i.e., high-value chemicals (HVC), cement, alumina, steel) and wastewater treatment plants benefit the most from the supply of electrolysis-derived oxygen, both in relative and absolute terms. Due to the high production volume of the HVC industry and the large wastewater volumes in wastewater treatment, these two applications offer the greatest absolute potential for the integration of electrolysis-derived oxygen.

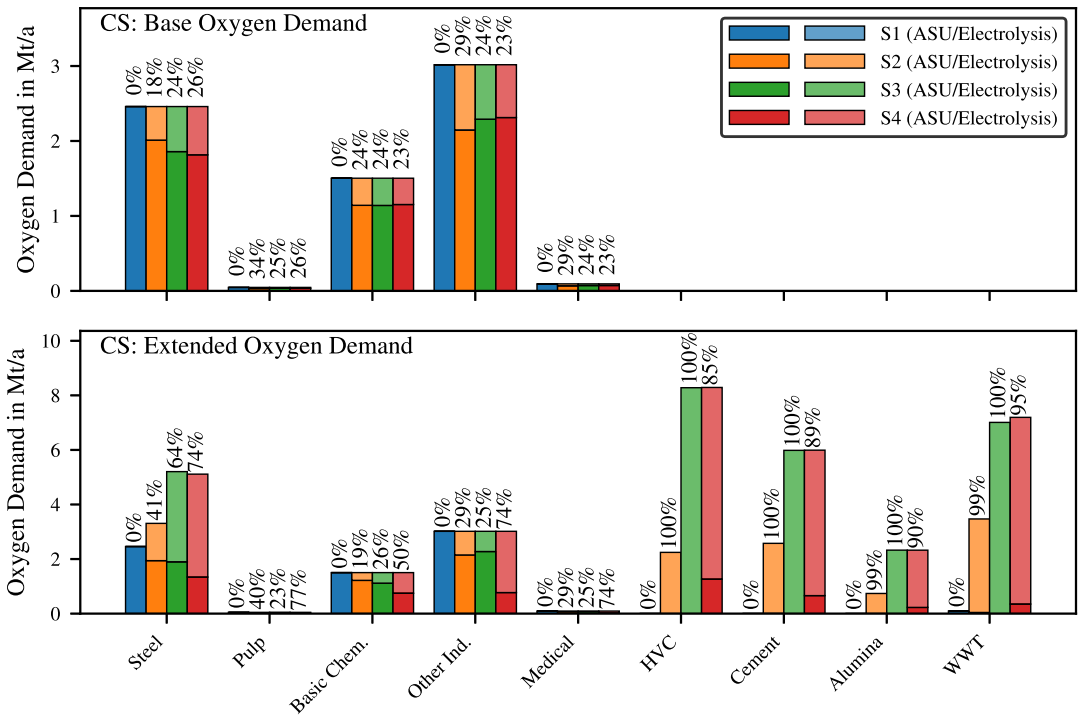

Fig. 8. Industrial oxygen demand and the proportionate supply from air separation units (ASU) and electrolysis for both case studies (CS). The color hue represents the scenario, with a lighter tint indicating oxygen supply via electrolysis and a darker shade indicating oxygen supply via ASU. The supply share from electrolysis is shown above the bars (HVC: High-Value Chemicals, WWT: Wastewater Treatment).

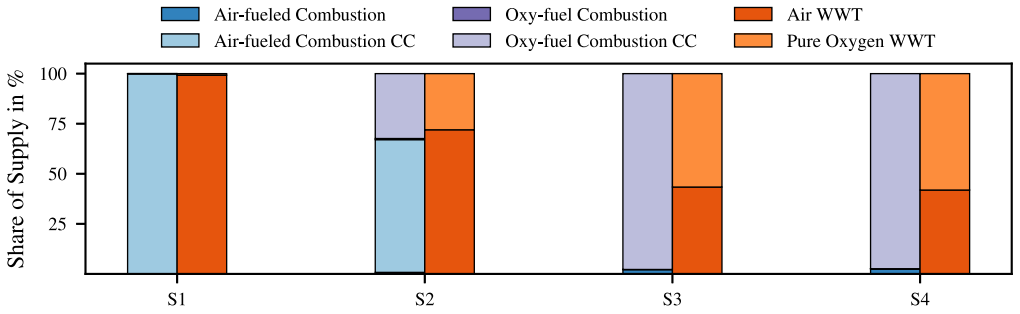

Fig. 9. Shares of the supply types in the industrial methane supply (blue, purple) and wastewater treatment (orange) for each of the four scenarios in the 'Extended Oxygen Demand' case study (CC: Carbon Capture, WWT: Wastewater Treatment).

4.2. Economic assessment

The economic analysis builds upon the infrastructure analysis. It first evaluates the total costs of the modeled German energy system in Section 4.2.1, followed by an examination of the levelized costs of oxygen and hydrogen in Section 4.2.2. The S1-scenario of the BOD case study serves as the reference case for the following comparisons, as it depicts the status quo of oxygen supply, reflecting current oxygen applications without accounting for electrolysis-derived oxygen.

4.2.1. Total costs

Fig. 10 illustrates the total annual costs of the modeled German energy system. The energy system model includes the entire electricity supply, industry, and transport sectors, with the oxygen supply constituting only a small fraction. Consequently, only modest relative cost reductions compared to total system costs are anticipated. Nonetheless, adopting a holistic perspective is crucial, as the utilization of electrolysis-derived oxygen can lead to cross-sectoral effects.

Base Oxygen Demand. Compared to the S1-scenario, total annual costs decrease across all subsequent scenarios. However, when the utilization of electrolysis-derived oxygen is not taken into account in the planning of electrolyzer deployment (as in S2), the reduction in total costs is negligible, amounting to only 0.01%. By slightly adjusting the siting of electrolyzers (see Figs. C.3 and C.7) and incorporating the utilization of electrolysis-derived oxygen (S3), a cost reduction of ca. 0.14% can be achieved. When both the oxygen and hydrogen supply infrastructures are redesigned simultaneously (S4), cost savings of ca. 0.17% are attainable. These findings indicate that, in principle, the integration of electrolysis-derived oxygen into existing oxygen applications is beneficial from a system-wide perspective. However, its overall impact on total system costs remains relatively modest in comparative terms.

Extended Oxygen Demand. In comparison to the reference case (S1 BOD), total costs in the S1-scenario of the EOD case study decrease by 0.11%, which is lower than the savings achieved in scenario S3 and higher than those in scenario S2 of the BOD case study. The conversion of individual wastewater treatment processes, which are supplied with oxygen from ASUs (see Section 4.1.3), is therefore cost-effective enough to outweigh the potential savings from the use of electrolysis-derived oxygen for existing oxygen applications, in the case that electrolysis oxygen utilization was not previously incorporated into the electrolyzer design.

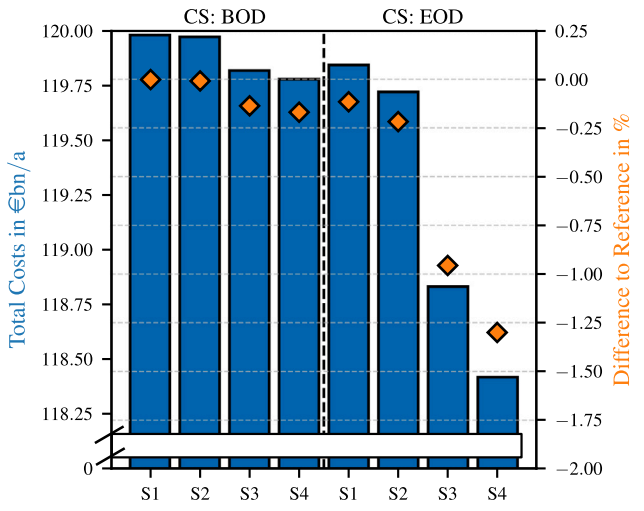

Fig. 10. Total costs of each scenario of the two case studies and the relative difference compared to the S1-scenario of the Base Oxygen Demand case study (reference) (CS: Case Study, BOD: Base Oxygen Demand, EOD: Extended Oxygen Demand).

However, total costs can be reduced by 0.22% in scenario S2, surpassing the savings in the best-case scenario of the BOD case study. This demonstrates that overall costs can be significantly reduced even if the utilization of electrolysis-derived oxygen is considered retrospectively, provided that expanded oxygen applications are developed. Nevertheless, the full potential of these applications is only realized when the utilization of electrolysis-derived oxygen is integrated into electrolyzer system design, yielding total cost savings of 0.96% (S3) and 1.3% (S4).

The development of new oxygen applications to maximize the utilization of excess oxygen from electrolysis offers significant cost-saving potential from a system-wide perspective. This potential arises from the ability to effectively integrate excess electrolyzer oxygen (in relation to the BOD case study) into the new EOD applications. Since the corresponding volumes of electrolysis-derived oxygen are produced either way as by-product, the associated oxygen supply costs for these applications are very low. As a result, the cost savings achieved through more efficient processes (i.e., methane savings in oxy-fuel applications and electricity savings in wastewater treatment) outweigh the minimal oxygen supply costs, leading to a net reduction in overall system costs. To fully capitalize on this potential, it is essential to account for oxygen use during the initial planning of hydrogen infrastructure.

4.2.2. Levelized costs

Fig. 11 illustrates the national levelized costs of oxygen (LCOO) and hydrogen (LCOH), broken down into their components for each scenario in the two case studies.

Base Oxygen Demand. Similar to the total costs, the LCOO progressively decrease across the scenarios, ranging from approximately 0.08 €/kg to 0.06 €/kg. This trend is driven by the integration of larger amounts of electrolysis-produced oxygen in each subsequent scenario (see Section 4.1.1). As a result, the reduced electricity consumption of the ASUs lowers their electricity costs since less oxygen is produced by the ASUs. However, this is accompanied by an increase in investment costs for oxygen storage tanks, which are required to balance the fluctuating production of electrolysis-derived oxygen with the industrial demand. The largest cost reduction occurs in scenario S4, where significant savings in ASU investment costs are realized due to the reduced ASU capacities (see Section 4.1.1).

For the BOD case study, the use of electrolysis-derived oxygen has a negligible impact on hydrogen infrastructure planning or hydrogen production from a national perspective (see Section 4.1.2). Furthermore, high oxygen surpluses result in low oxygen marginal prices. Combined with the relatively small absolute quantities of integrated electrolysis-derived oxygen, the utilization of electrolysis oxygen shows a minimal effect on the LCOH. Consequently, the total LCOH remain at ca. 3.3 €/kg across all scenarios.

Examining the deviation of the local LCOH relative to the corresponding S1-scenario (Fig. 12), similar to the national perspective, most local LCOH values are largely unaffected by the integration of electrolysis-derived oxygen. Due to slight capacity changes (see Fig. C.7), some sites exhibit minor reductions, while others show slight increases. However, changes of this magnitude may also result from numerical inaccuracies.

Extended Oxygen Demand. Scenario S1 shows a slight increase in the LCOO compared to the reference case (S1 BOD). This increase is attributed to higher CAPEX resulting from the expansion of ASU capacities and the addition of oxygen storage to support the extended oxygen applications at selected locations. For the other scenarios, a consistent trend of decreasing LCOO is observed, with even more pronounced cost reductions in these cases (0.02 to 0.08 €/kg). This is due to the increased integration of electrolysis-derived oxygen, allowing for greater substitution of ASU-produced oxygen (see Section 4.1.1). Consequently, the reduction in ASU electricity costs and the rise in oxygen storage investment costs are more significant. From scenario S2 to scenarios S3 and S4, the total oxygen demand increases significantly, while the quantities of oxygen produced from ASUs remain unchanged (see Section 4.1.1). This results in a further reduction in the LCOO, as per definition in Eq. (1).

The increased integration of electrolysis-derived oxygen also affects the national LCOH. In scenario S2, hydrogen demand decreases (see Section 4.1.1), while electrolysis capacities remain unchanged. This results in a proportionate increase in CAPEX and a reduction in electricity costs, leading to a slight overall decrease in the LCOH by ca. 0.1 €/kg. Additionally, the potential revenue from selling the oxygen produced exerts a further influence across the scenarios. This effect is particularly pronounced in scenarios, where electrolysis oxygen utilization is taken into account during the planning of the hydrogen infrastructure (S3, S4), where more decentralized electrolyzer locations (see Section 4.1.2) lead to fewer suitable sites for low-cost electricity generation. Although electricity costs increase in these scenarios, the revenue from oxygen sales more than compensates for the rise, resulting in a 7% reduction in LCOH, from 3.3 €/kg to slightly below 3.1 €/kg, compared to the reference case (S1 of the BOD case study).

The overall reduction in LCOH is also evident in the local variations in LCOH (Fig. 12), where nearly all sites exhibit at least slight reductions. Certain sites achieve significant LCOH reductions through the utilization of electrolysis-derived oxygen. However, a few sites experience an increase in LCOH. This is partly attributable to changes in electrolyzer capacities and hydrogen production volumes compared to scenario S1 (see Fig. C.7). The primary driver, however, is the rise in hydrogen storage costs. For example, at location 17, the LCOH including storage costs are 3.20 €/kg in scenario S1, compared to 3.02 €/kg without storage. In scenario S3, the LCOH increase to 4.48 €/kg with storage, while they are 3.00 €/kg without storage–representing a slight reduction relative to scenario S1 due to oxygen revenues. The increase in hydrogen storage costs — and the corresponding rise in storage capacity — can be attributed to two main factors. First, the specific storage costs for hydrogen are lower than those for oxygen, enabling better synchronization of electrolysis oxygen production and demand through hydrogen storage. This also explains the slight increase observed at location 17 in scenario S2. Second, the more decentralized deployment of electrolyzers leads to a shift in hydrogen production locations. From a system-wide perspective, this makes it more cost-effective to establish higher hydrogen storage capacities at other strategically selected sites to support a cost-efficient national hydrogen supply. While these specific cases offer economic benefits for the system as a whole, they pose economic disadvantages for the respective electrolyzer operations.

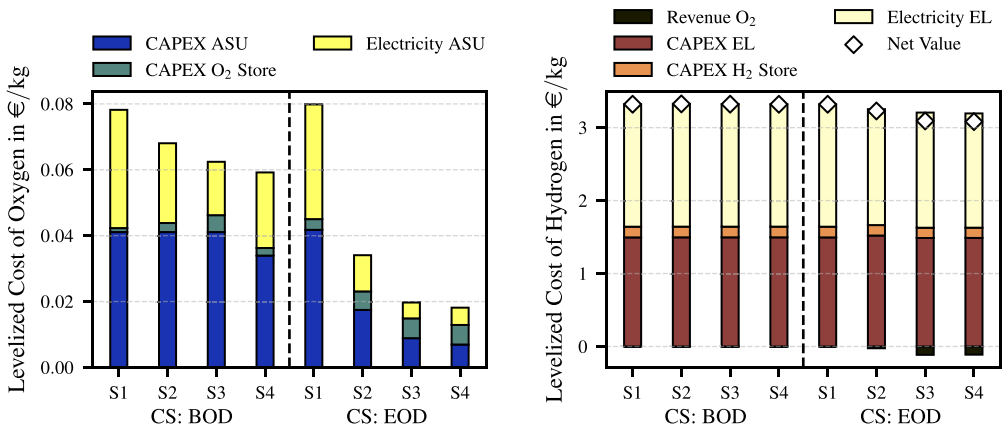

Fig. 11. National levelized costs of oxygen and hydrogen and their constituents for each scenario of the case studies (ASU: Air Separation Unit, EL: Electrolysis, CS: Case Study, BOD: Base Oxygen Demand, EOD: Extended Oxygen Demand).

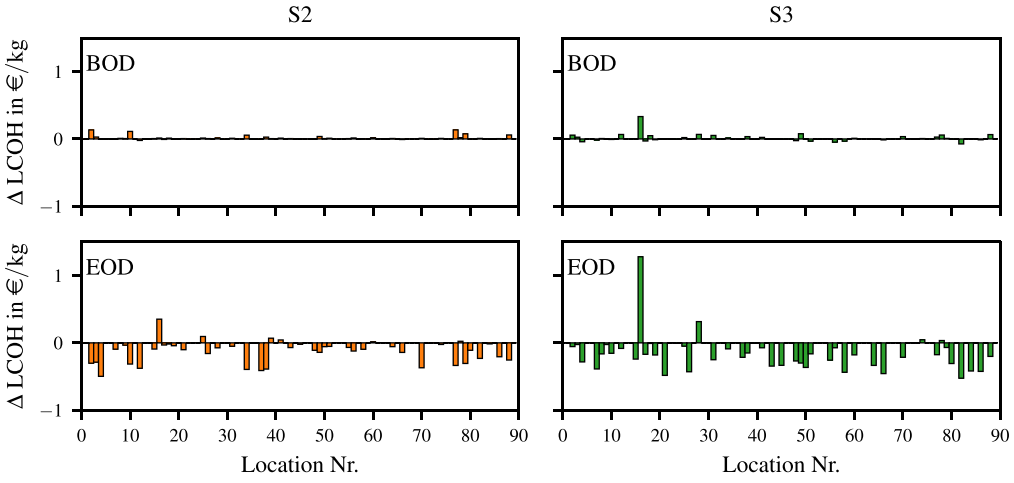

Fig. 12. Change of the nodal levelized costs of hydrogen (LCOH) for the S2- and S3-scenarios of the Base Oxygen Demand (BOD) and Extended Oxygen Demand (EOD) case studies. The change is in relation to the nodal LCOH of the respective S1-scenario. Locations with electrolyzer capacities < 2 MW are excluded for numerical reasons.

Consequently, a sufficiently high oxygen sales price is required to make this adjustment financially viable for the electrolyzer operator.

Since both LCOH and LCOO depend on electricity procurement costs and the utilization factors of the electrolyzers and ASUs, this relationship is visualized in Fig. C.9 in Appendix C.2.

5. Discussion

The integration of electrolyzer-derived oxygen into industrial applications presents both opportunities and challenges, depending on the scale of oxygen demand and the associated infrastructure. For current industrial oxygen applications, the results project a substantial surplus of oxygen from electrolyzers by 2045. However, the continued need for by-products such as argon from ASUs ensures that a baseline ASU capacity—and the associated oxygen production—remains necessary. As a result, only about 24% of industrial oxygen demand is met by electrolyzer-produced oxygen on average, leaving a significant portion unused. This limited utilization has minimal impact on hydrogen infrastructure design (i.e., the siting and capacities of electrolyzers) and does not incentivize hydrogen production beyond demand solely to use the by-product oxygen. While the sale of electrolyzer-derived oxygen might reduce the levelized cost of hydrogen (LCOH) at a few specific sites, its economic impact is negligible at most locations, making profitability highly site-dependent. Nevertheless, from a systemic perspective, integrating electrolyzer oxygen can reduce total costs within the German energy system, even under current industrial applications.

Expanding the scope of oxygen demand to include new industrial applications—such as oxy-fuel combustion in industrial processes and pure oxygen use in wastewater treatment—unlocks additional synergies. While these processes are often economically unviable when relying on ASU-derived oxygen due to insufficient overall cost savings compared to the electricity costs for the ASU, the integration of cost-effective electrolysis-derived oxygen increases their feasibility. To fully realize this potential, hydrogen infrastructure planning must consider the utilization of oxygen as by-product to ensure sufficient local production of oxygen via electrolysis to support these extended, cost-effective applications. Under such conditions, total system costs can be reduced by up to 1%, surpassing the cost benefits observed with current applications. Moreover, this approach provides a viable business case for electrolyzer operators, with LCOH decreasing on average by up to 7% across nearly all sites.

However, realizing these benefits requires a transition from centralized, large-scale electrolyzers — primarily sited in Northern Germany to capitalize on low-cost electricity from offshore wind — to smaller, decentralized units co-located with industrial sites. While decentralization enables local availability of oxygen for industrial processes, it may also result in higher electricity procurement costs, increased grid load, and relies on sufficiently high local oxygen demand and favorable pricing conditions to ensure economic viability. Despite these advances, a persistent surplus of electrolysis-derived oxygen remains — particularly as ca. 40% of wastewater treatment processes are not converted to pure oxygen operation — highlighting trade-offs between optimal electrolyzer siting and maximizing oxygen utilization.

From a system-cost perspective, redesigning the existing oxygen infrastructure could further enhance cost efficiency. By shifting ASUs to prioritize argon as their main product (with oxygen as a by-product), their strategic role would be redefined, with locations determined by cost minimization rather than direct oxygen demand. Building on this, a further step could involve replacing oxygen-based ASUs entirely with electrolyzers. In this context, industrial gases currently produced as by-products could either be substituted with alternative gases or, for instance, generated in ASUs where nitrogen is the primary product.

These findings underscore that while electrolyzer-derived oxygen offers significant systemic benefits and site-specific opportunities, its broader economic viability depends on careful alignment of infrastructure planning with localized demand conditions. Even in the EOD case study, with expanded applications and increased oxygen demand, a substantial share of electrolytic oxygen remains unused. The anticipated scale of hydrogen production—and the resulting by-product oxygen — exceeds projected oxygen demand. This oversupply challenges the economic viability of utilizing electrolytic oxygen. Low demand and high surpluses lead to reduced market prices, limiting the revenue potential for electrolyzer operators. Although increasing demand could raise market prices and improve profitability, this effect is constrained. As prices rise, some EOD applications (e.g., oxy-fuel combustion, wastewater treatment) become economically unviable, further limiting uptake and potentially reducing demand again. In conclusion, the ongoing surplus of electrolytic oxygen indicates that there is still untapped integration potential at the national level. Fully exploiting this potential will require the development of additional innovative oxygen applications. However, this search may be constrained not only by technical feasibility but also by economic factors, meaning that oxygen demand cannot be expanded without limits.

These results are based on an isolated modeling of the German energy system. This approach is chosen deliberately to ensure high local resolution, particularly at the industrial level. However, Germany's energy supply is part of a larger highly interconnected European energy system. As a result, optimal locations and capacities for electrolyzers may differ when considering a cost effective cross-border energy exchange with neighboring countries. Additionally, oxygen transportation between different nodes has been neglected, meaning that a production facility must be installed at least at every region where oxygen is needed. Consequently, very small ASUs and electrolyzers are sometimes modeled, though such small-scale installations would most likely not be viable in reality due to the high specific costs associated with such small plants. This limitation arises from the model's use of size-independent specific costs, which does not account for economies of scale. This restriction is necessary to limit computational effort, as otherwise a mixed-integer optimization would be required, which would render the optimization of such a complex energy system model computationally infeasible. In addition, the results outlined above are highly dependent on the underlying oxygen demand being strongly influenced by the predefined transformation pathways of the respective industries and the assumption that specific process-related oxygen demands will remain unchanged in the future. If alternative industrial process transformations occur, they could either positively or negatively affect the cost savings and their implications presented in this analysis.

6. Summary and conclusion

Hydrogen is gaining importance in the transition toward renewable energy, particularly as a clean fuel and energy storage solution. "Green" hydrogen, produced via electrolyzers powered by renewable sources, faces cost challenges, which could be partly offset by utilizing oxygen, a by-product of electrolysis. Thus, this study explores the potential of integrating electrolysis-derived oxygen into various industries to reduce overall system costs and optimize the hydrogen infrastructure.

Through a system-wide analysis based on a German energy system model, this paper evaluates how the incorporation of electrolysis-derived oxygen can improve economic viability for both the broader energy system and the hydrogen supply chain. The main findings can be summarized as follows.

- Under current conditions of industrial oxygen applications, substantial surpluses of oxygen from electrolyzers are expected to arise in the future, which cannot be fully integrated given existing demand patterns. Since the conventional oxygen supply remains essential for the provision of co-produced industrial gases (e.g., argon)—at least in the absence of suitable substitutes—redefining these by-products as main products allows only approximately 24% of the total industrial oxygen demand to be met by electrolyzers under cost-optimal conditions. Nevertheless, this partial integration can lead to overall system cost reductions of up to 0.2%, without significantly affecting the levelized cost of hydrogen (LCOH) or the hydrogen infrastructure with regard to electrolyzer siting and installed capacity.
- Greater synergies can be achieved if additional oxygen applications are introduced, resulting in total system cost reductions of up to 1.3% and LCOH reductions of up to 7% on average. To realize this cost-effectiveness, electrolysis oxygen utilization needs to be taken into consideration during planning of the hydrogen infrastructure. Under these assumptions, electrolyzer siting would be driven primarily by industrial oxygen demand rather than optimal electricity procurement conditions.
- Among existing industrial oxygen applications, the steel industry particularly benefits from the use of electrolysis-derived oxygen. In addition, wastewater treatment and high-value chemical industries represent the most promising new applications, offering significant opportunities for system-beneficial integration of electrolysis oxygen.

In summary, this paper highlights the future potential of electrolysis-derived oxygen to achieve systemic cost reductions and enhance the cost-efficiency of hydrogen production. To fully realize this potential, it is recommended that electrolyzer operators account for oxygen utilization early in the planning and siting stages. Furthermore, reviewing industrial processes to assess whether incorporating pure oxygen from nearby electrolyzers could improve process efficiency may yield additional system-wide benefits.

CRediT authorship contribution statement

Luka Bornemann: Methodology, Software, Conceptualization, Writing – original draft, Data curation, Visualization, Formal analysis. **Jelto Lange:** Writing – review & editing, Conceptualization, Supervision. **Martin Kaltschmitt:** Supervision, Writing – review & editing, Funding acquisition, Conceptualization.

Declaration of competing interest

The authors declare that they have no known competing financial interests or personal relationships that could have appeared to influence the work reported in this paper.

Declaration of Generative AI and AI-assisted technologies in the writing process

During the preparation of this work the authors used ChatGPT in order to improve readability and language. After using this tool/service, the authors reviewed and edited the content as needed and take full responsibility for the content of the publication.

Acknowledgments

This research is supported by the German Federal Ministry for Economic Affairs and Climate Action under the 'Green hydrogen for Lübeck's mobility of tomorrow - Hydrogen supply for the operation of a waste collection vehicle under a holistic use of all side streams - Subproject Modeling and Assessment' (HyHL) project with the funding code 03EI3055D. Furthermore, the authors express their gratitude to Vincent Rode and thank him for his helpful cooperation in the preparation of the methodological approach for this paper.

Appendix A. Energy system model

This section provides a concise overview of the mathematical formulation underlying PyPSA-Eur. For a comprehensive explanation of the model, readers are directed to the original literature (e.g., [21,38,39]).

PyPSA-Eur employs a linear optimization framework to determine the energy system configuration that minimizes annual system costs, as defined by the objective function in Eq. (A.1) [2]. In this formulation, $G_{i,\gamma}$ represents the installed capacity of generation technology $\gamma \in \Gamma$ at bus $i \in \mathcal{I}$, while $S_{i,\sigma}$ denotes the storage capacity of technology $\sigma \in \Sigma$. The capacities of electricity transmission lines at line $j \in \mathcal{J}$ and energy conversion or transport infrastructure (e.g., hydrogen pipelines and electrolyzers) at link $k \in \mathcal{K}$ are represented by L_j and T_k, respectively. Additionally, $g_{i,\gamma,\tau}$ indicates the dispatch of generators, and $t_{k,\tau}$ represents the dispatch of links at time step $\tau \in \mathcal{T}$.

The cost terms incorporated into the optimization include annualized investment costs c and operating costs o, both considered for each technology. If the selected temporal resolution exceeds one hour, operating costs are weighted by a factor w_τ, ensuring that the total weighted time steps $|\mathcal{T}|\, w_\tau$ sum to 8760 h.

$$\begin{aligned}\min_{\boldsymbol{G},\boldsymbol{S},\boldsymbol{L},\boldsymbol{T},\boldsymbol{g},\boldsymbol{t}} & \sum_{i\in\mathcal{I}}\left(\sum_{\gamma\in\Gamma} c_{i,\gamma}G_{i,\gamma} + \sum_{\sigma\in\Sigma} c_{i,\sigma}S_{i,\sigma}\right) \\ & + \sum_{j\in\mathcal{J}} c_j L_j + \sum_{k\in\mathcal{K}} c_k T_k \\ & + \sum_{t\in\mathcal{T}} w_\tau \left(\sum_{i\in\mathcal{I}}\sum_{\gamma\in\Gamma} o_{i,\gamma}g_{i,\gamma,\tau} + \sum_{k\in\mathcal{K}} o_k t_{k,\tau}\right)\end{aligned} \tag{A.1}$$

The model incorporates a series of linear constraints governing various system components. For instance, the capacities of generators, storage units, electricity transmission lines, and other infrastructure elements are restricted within a range between the currently installed capacity and an upper bound reflecting the maximum feasible expansion. This constraint is exemplified in Eq. (A.2) for generator components $G_{i,\gamma}$ [2]:

$$\underline{G}_{i,\gamma} \le G_{i,\gamma} \le \overline{G}_{i,\gamma} \quad \forall i \in \mathcal{I}, \gamma \in \Gamma \tag{A.2}$$

Here, $\underline{G}_{i,\gamma}$ represents the minimum allowable generator capacity (e.g., existing installations of a specific technology), while $\overline{G}_{i,\gamma}$ denotes the upper limit, which depends on factors such as land availability for renewable energy deployment. Not all technologies are subject to this upper bound. Additionally, operational constraints apply, particularly for generator dispatch. Eq. (A.3) expresses this limitation, where $\underline{g}_{i,\gamma,\tau}$ defines a time-dependent minimum utilization, and $\overline{g}_{i,\gamma,\tau}$ represents the maximum availability (e.g., weather-dependent capacity factors for wind and solar power) [2]:

$$\underline{g}_{i,\gamma,\tau} G_{i,\gamma} \le g_{i,\gamma,\tau} \le \overline{g}_{i,\gamma,\tau} G_{i,\gamma} \quad \forall i \in \mathcal{I}, \gamma \in \Gamma, \tau \in \mathcal{T} \tag{A.3}$$

Similarly, energy storage levels are constrained by the installed capacity $S_{i,\sigma}$, as shown in Eq. (A.4). The variable $s_{i,\sigma,\tau}$ represents the stored energy in technology σ at time step τ at bus i [2]:

$$0 \le s_{i,\sigma,\tau} \le S_{i,\sigma} \quad \forall i \in \mathcal{I}, \sigma \in \Sigma, \tau \in \mathcal{T} \tag{A.4}$$

Stored energy levels evolve over time according to Eq. (A.5), which accounts for self-discharge at a rate of $\eta_{i,\sigma}^{w_\tau}$ and the net charging or discharging process, represented by $\epsilon_{i,\sigma,\tau}$ [2]:

$$s_{i,\sigma,\tau} = s_{i,\sigma,\tau-1}\eta_{i,\sigma}^{w_\tau} + w_\tau \epsilon_{i,\sigma,\tau} \quad \forall i \in \mathcal{I}, \sigma \in \Sigma, \tau \in \mathcal{T} \tag{A.5}$$

One of the fundamental constraints in the optimization ensures that the system meets the (inflexible) energy demand $d_{i,\tau}$ at every time step. A simplified version of this condition is given in Eq. (A.6) [2]:

$$\sum_{\gamma\in\Gamma} g_{i,\gamma,\tau} + \sum_{\sigma\in\Sigma} \epsilon_{i,\sigma,\tau} + \sum_{j\in\mathcal{J}} \boldsymbol{K}_{ij} l_{j,\tau} + \sum_{k\in\mathcal{K}} \boldsymbol{K}_{ik\tau} t_{k,\tau} = d_{i,\tau} \quad \forall i \in \mathcal{I}, \tau \in \mathcal{T} \tag{A.6}$$

Apart from technology-specific generation and storage operations at each bus i and time step τ, local energy demand is also met through energy transport via transmission lines and links. The power flow through transmission lines, denoted by $l_{j,\tau}$, is weighted by the incidence matrix $\boldsymbol{K}_{ij}$, which contains entries of 1 and −1 to indicate line start and end points. Similarly, link-based energy transfer is captured using $t_{k,\tau}$, scaled by the lossy incidence matrix $\boldsymbol{K}_{ik\tau}$, which incorporates efficiency values $\eta_{i,k,\tau}$ instead of unitary coefficients for links terminating at bus i [2]. Beyond constraints related to individual technologies, PyPSA-Eur also imposes system-wide restrictions, such as a cap on total annual CO_2 emissions. Eq. (A.7) expresses this limitation, where ρ_γ represents the specific emissions of each generation technology γ, and Λ_{CO2} defines the maximum allowable CO_2 emissions for the entire system [2]:

$$\sum_{i\in\mathcal{I},\gamma\in\Gamma,\tau\in\mathcal{T}} \rho_\gamma w_\tau g_{i,\gamma,\tau} \le \Lambda_{\mathrm{CO_2}} \tag{A.7}$$

Appendix B. Model setup

Further system assumptions and more detailed information on the case studies are outlined below.

B.1. System assumptions and framework conditions

Table B.1 shows techno-economic parameters of the oxygen-related energy system components.

The techno-economic data for all hydrogen components are already integrated into PyPSA-Eur. These data are derived from various primary sources, account for the respective reference year, and have undergone multiple peer reviews. Therefore, no manual modifications are made in this study.

The electrolysis component in PyPSA-Eur does not distinguish between different electrolyzer technologies. However, the underlying techno-economic data are largely based on alkaline electrolyzers. Alkaline electrolyzers currently represent the most mature electrolyzer technology, characterized by an operating temperature of 60 to 90 °C, low current densities, and low load flexibility, with investment costs ranging from 800 to 1500 €/kW. In addition to alkaline systems, polymer electrolyte membrane (PEM) electrolyzers are considered as a particularly promising technology. Compared to alkaline electrolyzers, PEM electrolyzers operate at lower temperatures (50 to 80 °C), support higher current densities and greater load flexibility, making them particularly attractive for integration into energy systems – albeit currently at higher investment costs of 1400 to 2100 €/kW [3].

Other studies project significantly more optimistic cost developments for electrolyzers. Depending on the technology, investment costs could decline by 2050 to as low as 330 USD/kW (alkaline) and 437 USD/kW (PEM) [44]. However, these projections often assume both a significantly faster hydrogen scale-up and more rapid technological advancements in electrolyzer technologies than have been observed in recent years. It is therefore uncertain whether such optimistic economic assumptions will materialize.

As shown in Eqs. (1) and (2), investment costs have a substantial impact on both LCOH and LCOO. However, this study does not aim to provide universally valid absolute values for LCOH and LCOO,

Table B.1
Techno-economic parameters of the oxygen-related energy system components. The parameters of the argon storage are based on a generic CO_2 storage tank (ASU: Air Separation Unit).

Component	ASU	Oxygen Storage	Argon Storage	Electrolyzer
CAPEX	2.92 M€/(t_{O_2} h)	1670 €/t_{O_2}	2584 €/t_{Ar}	1100 €/kW_{el}
OPEX	4%	1%	1%	4%
Lifetime	25 a	25 a	25 a	25 a
Electricity demand	370 kWh_{el}/t_{O_2} [a]			1.53 kWh_{el}/kWh_{H_2}
References	[14,40,41]	[42,43]	[42]	[42]

[a] Based on Air Liquide SIGMA plant [14].

Table B.2
Parameter for determining the per capita oxygen and electricity demands for wastewater treatment [17] and oxy-fuel combustion.

Parameter	Value	Unit
$BOxD$	300	mg/L
q_{avg}	250	L/(d pers)
$SOTE$	20	%
p_{wwt,O_2}	80	kWh/t_{O_2}
$p_{wwt,air}$	407	kWh/t_{O_2}
$P_{el,air}^{wwt,an}$	55.67	kWh/(a pers)
$P_{el,O_2}^{wwt,an}$	10.96	kWh/(a pers)
$D_{O_2}^{oxy,CH_4}$	0.288	t_{O_2}/MWh_{CH_4}

Table B.3
Techno-economic parameters of the extended oxygen-related energy system components (CC: Carbon Capture, WWT: Wastewater Treatment).

Component		Combustion		WWT	
		Oxy-fuel	Oxy-fuel CC	Air	Pure Oxygen
CAPEX	M€/(t_{CO_2} h)	0.47	2.7		
OPEX	$\%_{CAPEX}$	3	3		
Lifetime	a	25	25		
Electricity Demand	kWh/(pers a)			55.76	10.96
Oxygen Demand	t_{O_2}/(pers a)				0.147
Fuel Reductions	%		20		
Carbon Capture Rate	%		95		
References		[41]	[41]	[17]	[17]

but rather to examine overall system-level effects and their relative influence on total system costs, as well as on LCOH and LCOO. While the assumed investment cost levels do influence the results, their role is secondary in this context due to the consistent input data used for all scenarios.

A central requirement of this study is the reflection of realistic hydrogen applications and, above all, production volumes within the optimization framework. According to projections by the German Federal Ministry for Economic Affairs and Climate Protection, domestic hydrogen production is expected to reach 190 to 245 TWh, supported by an electrolyzer capacity of 80 to 100 GW [45]. Within this work, across all scenarios and case studies, a domestic hydrogen production of 195 TW h and an electrolyzer capacity of 63 GW is projected, which are within a realistic range compared to the projections by the German Federal Ministry for Economic Affairs and Climate Protection. Consequently, these values provide a meaningful basis for analyzing future hydrogen and oxygen availability.

Varying the assumed investment costs — particularly by reducing them — would likely result in a more extensive expansion of the hydrogen infrastructure, potentially leading to an overestimation of future hydrogen and oxygen availability. Therefore, no further differentiation or variation of electrolyzer investment costs is conducted in this study.

B.2. Case studies: Extended oxygen demand

The specific oxygen demand for oxy-fuel combustion of methane $D_{O_2}^{oxy,CH_4}$ is calculated based on the lower heating value of methane LHV_{CH_4} (as defined in PyPSA-Eur) and the ratio of the molar masses M_i to the stoichiometric molar quantities n_i of oxygen and methane ($\forall i \in \{O_2, CH_4\}$), as shown in Eq. (B.1).

$$D_{O_2}^{oxy,CH_4} = \frac{M_{O_2}}{LHV_{CH_4}\ M_{CH_4}} \frac{n_{O_2}}{n_{CH_4}} \tag{B.1}$$

The annual oxygen demand for wastewater treatment $D_{O_2}^{wwt,an}$ is calculated using the biochemical oxygen demand $BOxD$, the average per capita wastewater production rate q_{avg} and the standard oxygen transfer efficiency $SOTE$ (Eq. (B.2)).

$$D_{O_2}^{wwt,an} = \frac{BOxD\ q_{avg}}{SOTE} 365\,d/a \tag{B.2}$$

The annual power demand for wastewater treatment $P_{el,i}^{wwt,an}$ is then determined based on the specific power requirement of the blowers used for oxygen input $p_{wwt,i}$ ($\forall i \in \{air, O_2\}$, Eq. (B.3)).

$$P_{el,i}^{wwt,an} = D_{O_2}^{wwt,an} p_{wwt,i} \tag{B.3}$$

The corresponding parameters can be found in Table B.2.

Table B.3 shows the techno-economic parameters of oxy-fuel combustion and wastewater treatment processes integrated into the existing model.

Appendix C. Further results

Further results of the case studies and scenarios examined are presented below.

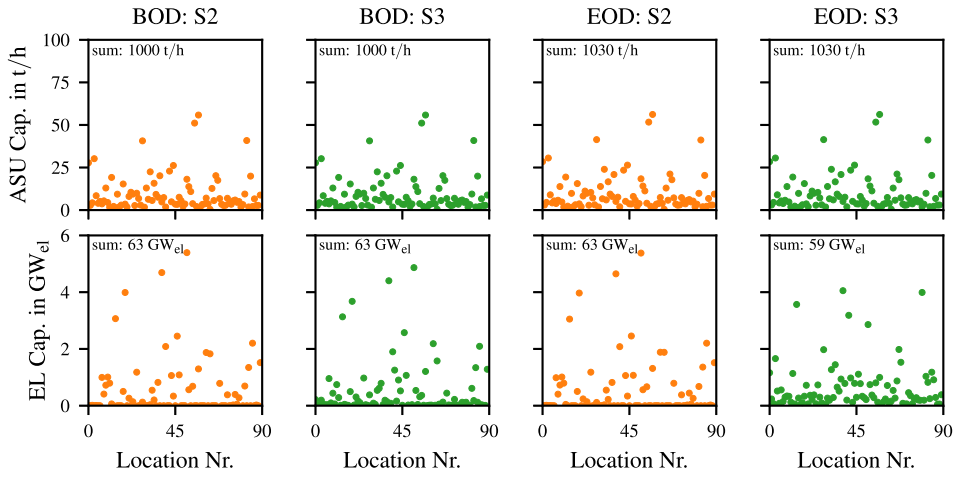

Fig. C.1. Installed capacity of the air separation unit (ASU) and electrolysis (EL) in each node under consideration for scenarios S2 and S3 of both case studies (BOD: Base Oxygen Demand, EOD: Extended Oxygen Demand).

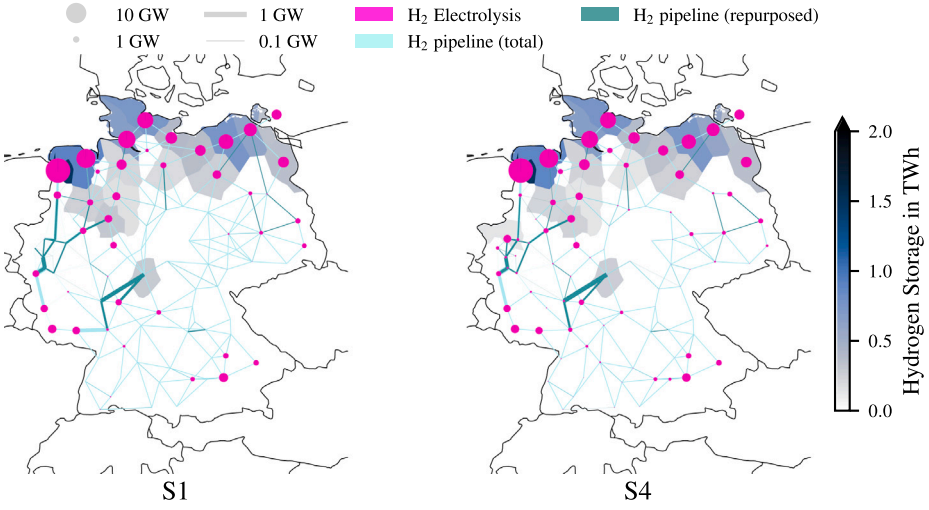

Fig. C.2. Map of Germany for the 'Base Oxygen Demand' case study for scenario S1 and S4. The local electrolysis and hydrogen storage capacities as well as the expansion of the hydrogen network pipelines are shown.

C.1. Infrastructure assessment

Figs. C.1 to C.7 show the local capacities of the air separation units and electrolyzers of the scenarios that were not analyzed in the main section. Fig. C.8 shows a production map of the different industries for reference.

C.2. Levelized costs

Fig. C.9 presents the levelized costs of hydrogen (LCOH) and oxygen (LCOO) as a function of the levelized costs of electricity (LCOE) and the capacity factors of electrolyzers (for LCOH) and ASUs (for LCOO) across all nodes in both case studies for the corresponding scenario S3. The LCOE represent annual averages for the respective node/location. For this, the local electricity marginal prices $c_{n,t,el}$ are weighted by the electricity consumption of the electrolyzers or the ASU $\dot{E}^{c}_{n,t,el}$ ($\forall c \in \{EL, ASU\}$), ensuring that operating hours and production volumes are appropriately reflected in the calculated LCOE (Eq. (C.1)).

$$LCOE_{n,c} = \frac{\sum_{t\in\mathcal{T}} c_{n,t,el}\,\dot{E}^{c}_{n,t,el}}{\sum_{t\in\mathcal{T}} \dot{E}^{c}_{n,t,el}}, \quad \forall c \in \{EL, ASU\} \tag{C.1}$$

The results confirm that both LCOH and LCOO increase with rising LCOE and decrease with increasing capacity factor. However, it is evident that electrolyzers operate only within an LCOE range of 22 to 42 €/MWh and capacity factors between 40 to 70%, regardless of the case study. In contrast, ASU operation differs between the case studies: in the BOD case study, ASUs are operated at LCOEs ranging from 50 to 80 €/MWh and capacity factors between 70 to 90%, whereas in the EOD case study, LCOEs span from 20 to 90 €/MWh with capacity factors between 40 to 90%.

The following conclusions can be drawn: Due to their lower capacity factors, electrolyzers offer greater operational flexibility, allowing them

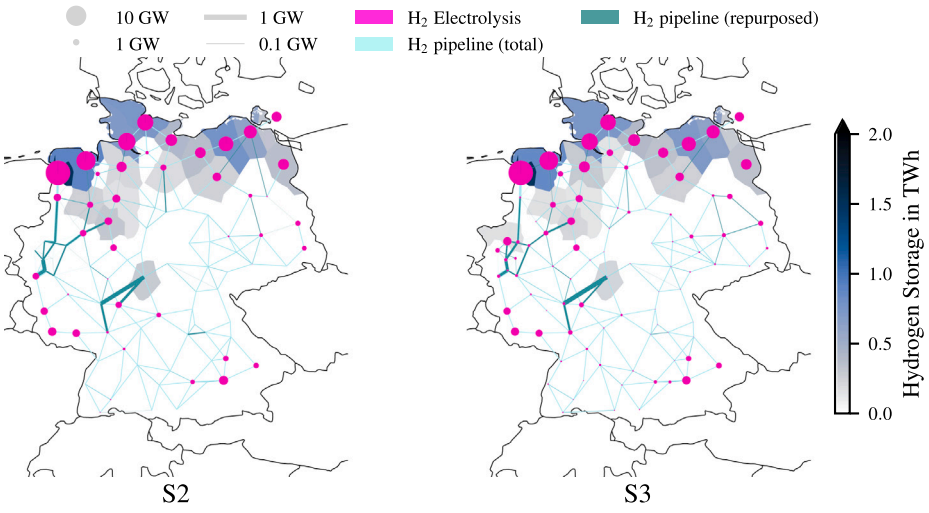

Fig. C.3. Map of Germany for the 'Base Oxygen Demand' case study for scenarios S2 and S3. The local electrolysis and hydrogen storage capacities as well as the expansion of the hydrogen network pipelines are shown.

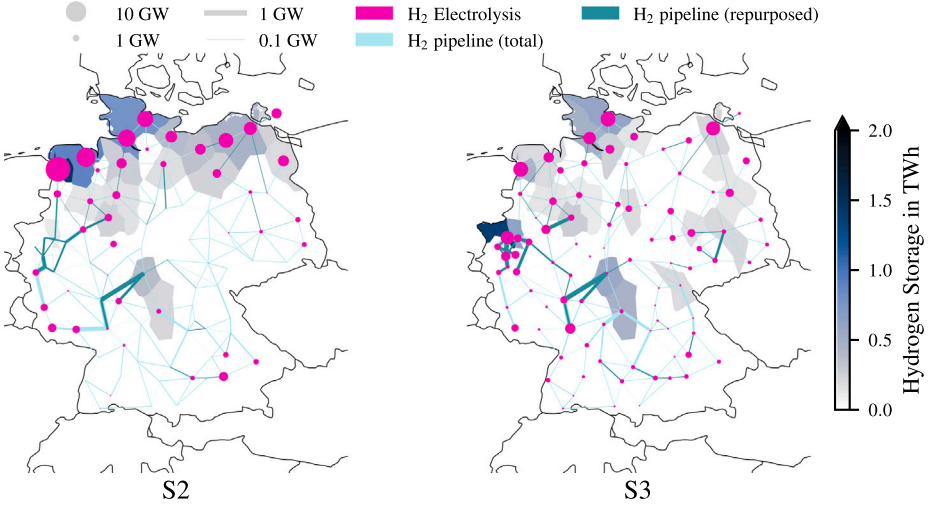

Fig. C.4. Map of Germany for the 'Extended Oxygen Demand' case study for scenarios S2 and S3. The local electrolysis and hydrogen storage capacities as well as the expansion of the hydrogen network pipelines are shown.

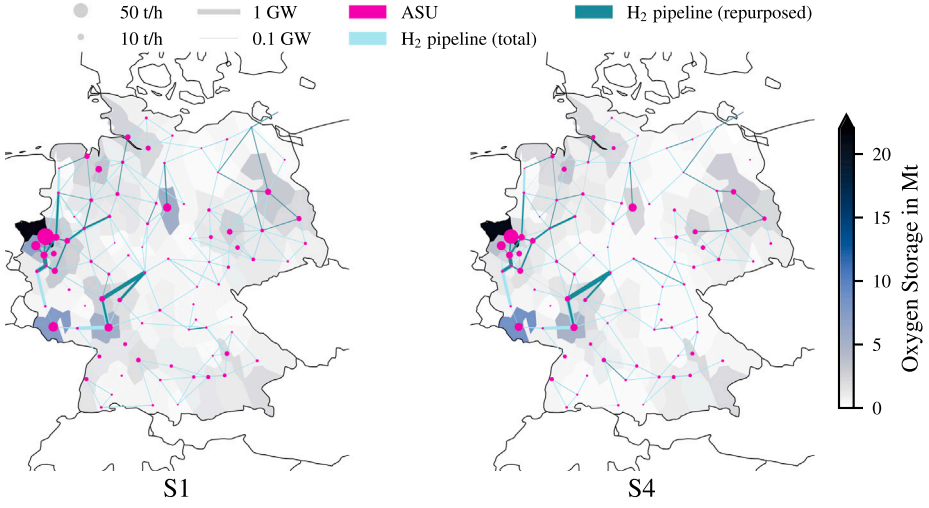

Fig. C.5. Map of Germany for the 'Base Oxygen Demand' case study for scenarios S1 and S4. The local air separation unit (ASU) and oxygen storage capacities as well as the expansion of the hydrogen network pipelines are shown.

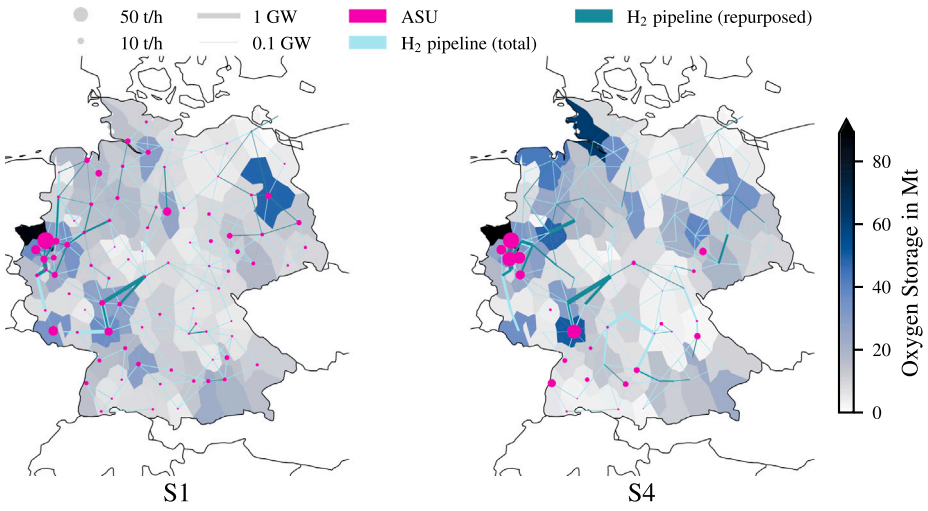

Fig. C.6. Map of Germany for the 'Extended Oxygen Demand' case study for scenarios S1 and S4. The local air separation unit (ASU) and oxygen storage capacities as well as the expansion of the hydrogen network pipelines are shown.

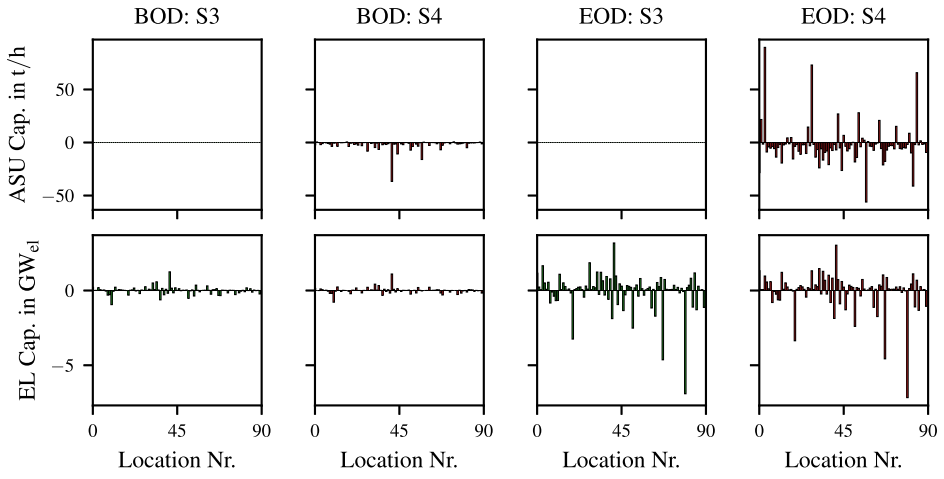

Fig. C.7. Difference in installed capacity of the air separation unit (ASU) and electrolysis (EL) in each node under consideration for the scenarios S3 and S4, compared to the respective S1-scenario of both case studies (BOD: Base Oxygen Demand, EOD: Extended Oxygen Demand).

to better align production with periods of low electricity prices. In contrast, the high capacity factors of ASUs — particularly in the BOD case study — indicate limited operational flexibility, necessitating oxygen production even during periods of higher electricity prices.

As discussed in Section 4.1, the more decentralized deployment of electrolyzers in the EOD case study leads to ASUs being used more as a supplemental oxygen source. At some sites, this results in lower capacity utilization and therefore greater flexibility to respond to low electricity prices. At other sites, higher capacity utilization limits this flexibility, requiring oxygen production even when electricity prices are elevated.

Data availability

The code for the energy system model, along with the results and input data used in this study, is available in a Zenodo repository at https://zenodo.org/records/15167498 under the MIT license.

Code and Data for Paper: Oxygen Production via Electrolysis: A Model-Based Assessment of Its Impact on a Climate-Neutral German Energy System (Original data) (Zenodo)

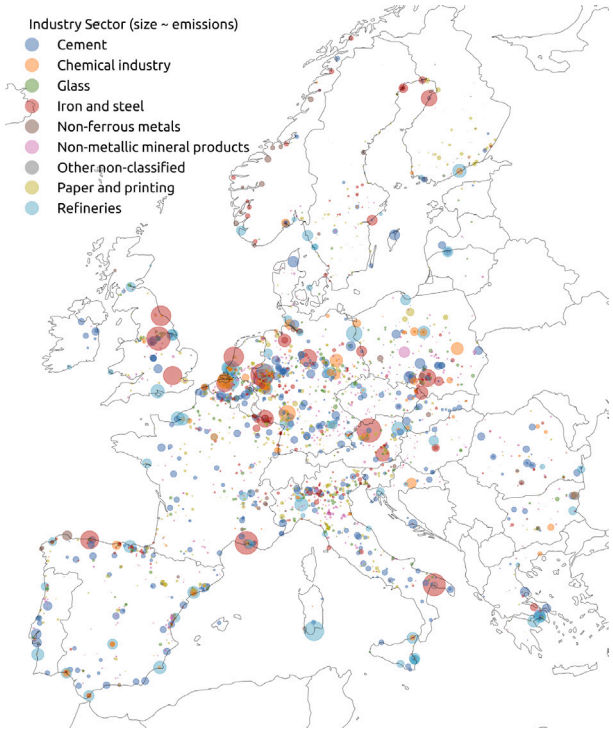

Fig. C.8. Local industry production emissions [46].

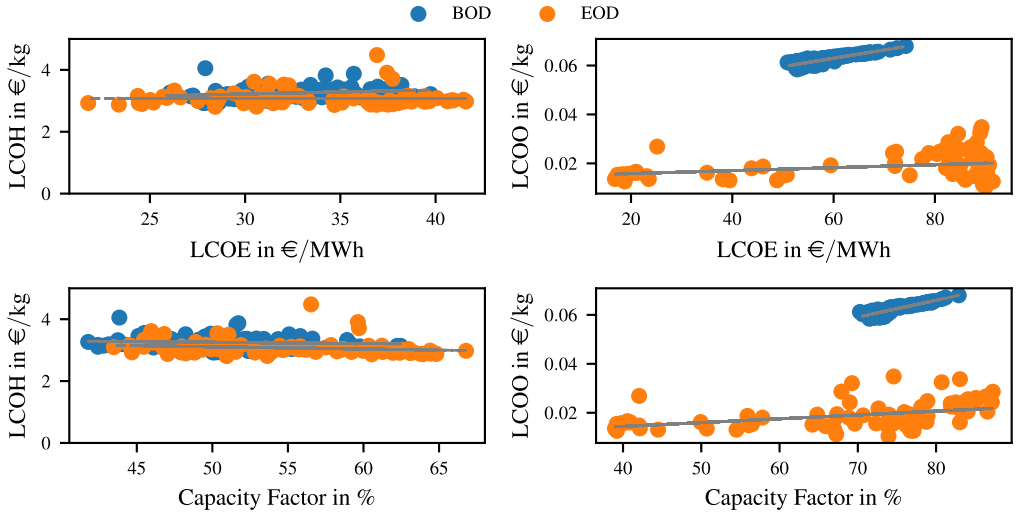

Fig. C.9. Levelized costs of hydrogen (LCOH) and oxygen (LCOO) as a function of the levelized costs of electricity (LCOE) and capacity factor of electrolyzers (LCOH) and air separation units (LCOO) across all nodes in both case studies, exemplified for the corresponding S3 scenario (BOD: Base Oxygen Demand, EOD: Extended Oxygen Demand).

References

[1] Squadrito G, Maggio G, Nicita A. The green hydrogen revolution. Renew Energy 2023;216:119041. http://dx.doi.org/10.1016/j.renene.2023.119041.

[2] Lange J, Schulthoff M, Puszkiel J, Sens L, Jepsen J, Klassen T, et al. Aboveground hydrogen storage – Assessment of the potential market relevance in a Carbon-Neutral European energy system. Energy Convers Manage 2024;306:118292. http://dx.doi.org/10.1016/j.enconman.2024.118292.

[3] Buttler A, Spliethoff H. Current status of water electrolysis for energy storage, grid balancing and sector coupling via power-to-gas and power-to-liquids: A review. Renew Sustain Energy Rev 2018;82:2440–54. http://dx.doi.org/10.1016/j.rser.2017.09.003.

[4] Sens L, Piguel Y, Neuling U, Timmerberg S, Wilbrand K, Kaltschmitt M. Cost minimized hydrogen from solar and wind – Production and supply in the European catchment area. Energy Convers Manage 2022;265:115742. http://dx.doi.org/10.1016/j.enconman.2022.115742.

[5] Karl A, Jodat E, Kungl H, Dobrenizki L, Schmid G, Geskes P, Eichel R-A. Water electrolysis facing the gigawatt challenge—comprehensive de-risking of proton exchange membrane and anion exchange membrane electrolyser technology. Electrochem Sci Adv 2025;n/a(n/a):e202400041. http://dx.doi.org/10.1002/elsa.202400041.

[6] Wappler M, Unguder D, Lu X, Ohlmeyer H, Teschke H, Lueke W. Building the green hydrogen market – Current state and outlook on green hydrogen demand and electrolyzer manufacturing. Int J Hydrog Energy 2022;47(79):33551–70. http://dx.doi.org/10.1016/j.ijhydene.2022.07.253.

[7] Ravkina O. Dezentrale sauerstoffproduktion. Technical Report, Fraunhofer IKTS; 2022.

[8] Hegemann K-R, Guder R. Stahlerzeugung. Wiesbaden: Springer Fachmedien Wiesbaden; 2020, http://dx.doi.org/10.1007/978-3-658-29091-7.

[9] Kuparinen K, Vakkilainen E, Ryder P. Integration of electrolysis to produce hydrogen and oxygen in a pulp mill process. Appita: Technol Innov Manuf Environ 2016;69(1):81–8.

[10] Squadrito G, Nicita A, Maggio G. A size-dependent financial evaluation of green hydrogen-oxygen co-production. Renew Energy 2021;163:2165–77. http://dx.doi.org/10.1016/j.renene.2020.10.115.
[11] Maggio G, Squadrito G, Nicita A. Hydrogen and medical oxygen by renewable energy based electrolysis: A green and economically viable route. Appl Energy 2022;306:117993. http://dx.doi.org/10.1016/j.apenergy.2021.117993.
[12] Hurskainen M. Industrial oxygen demand in Finland. Lappeenranta, Finland: Technical Research Centre of Finland VTT Ltd.; 2017,
[13] Chorowski M, Gizicki W. Technical and economic aspects of oxygen separation for oxy-fuel purposes. Arch Thermodyn 2015;36(1):157–70. http://dx.doi.org/10.1515/aoter-2015-0011.
[14] Šulc R, Ditl P. A technical and economic evaluation of two different oxygen sources for a small oxy-combustion unit. J Clean Prod 2021;309:127427. http://dx.doi.org/10.1016/j.jclepro.2021.127427.
[15] Assunção R, Eckl F, Ramos CP, Correia CB, Neto RC. Oxygen liquefaction economical value in the development of the hydrogen economy. Int J Hydrog Energy 2024;62:109–18. http://dx.doi.org/10.1016/j.ijhydene.2024.02.205.
[16] Del Furszyfer Rio DD, Sovacool BK, Foley AM, Griffiths S, Bazilian M, Kim J, et al. Decarbonizing the glass industry: A critical and systematic review of developments, sociotechnical systems and policy options. Renew Sustain Energy Rev 2022;155:111885. http://dx.doi.org/10.1016/j.rser.2021.111885.
[17] Mohammadpour H, Cord-Ruwisch R, Pivrikas A, Ho G. Utilisation of oxygen from water electrolysis – Assessment for wastewater treatment and aquaculture. Chem Eng Sci 2021;246:117008. http://dx.doi.org/10.1016/j.ces.2021.117008.
[18] Rusmanis D, Yang Y, Lin R, Wall DM, Murphy JD. Operation of a circular economy, energy, environmental system at a wastewater treatment plant. Adv Appl Energy 2022;8:100109. http://dx.doi.org/10.1016/j.adapen.2022.100109.
[19] Nhuchhen DR, Sit SP, Layzell DB. Decarbonization of cement production in a hydrogen economy. Appl Energy 2022;317:119180. http://dx.doi.org/10.1016/j.apenergy.2022.119180.
[20] Dashtizadeh E, Houshfar E. Multi-objective optimization and 4E analysis of a multigeneration system for hydrogen production using WHR in cement plants. Results Eng 2025;25:103845. http://dx.doi.org/10.1016/j.rineng.2024.103845.
[21] Neumann F, Zeyen E, Victoria M, Brown T. The potential role of a hydrogen network in Europe. Joule 2023;7(8):1793–817. http://dx.doi.org/10.1016/j.joule.2023.06.016.
[22] German Federal Government. Climate change act 2021. 2021.
[23] Hörsch J, Hofmann F, Schlachtberger D, Neumann F, Brown T, Hampp J. Weather data cutouts for PyPSA-eur: an open optimisation model of the European transmission system. 2024, http://dx.doi.org/10.5281/ZENODO.12791128.
[24] Pfeifroth U, Kothe S, Müller R, Trentmann J, Hollmann R, Fuchs P, et al. Surface radiation data set - heliosat (SARAH). 2nd ed.. Satellite Application Facility on Climate Monitoring (CM SAF); 2017, p. 7.1 TiB. http://dx.doi.org/10.5676/EUM_SAF_CM/SARAH/V002.
[25] Hersbach H, Bell B, Berrisford P, Hirahara S, Horányi A, Muñoz-Sabater J, et al. The ERA5 global reanalysis. Q J R Meteorol Soc 2020;146(730):1999–2049. http://dx.doi.org/10.1002/qj.3803.
[26] Lechtenböhmer S, Nilsson LJ, Åhman M, Schneider C. Decarbonising the energy intensive basic materials industry through electrification – implications for future EU electricity demand. Energy 2016;115:1623–31. http://dx.doi.org/10.1016/j.energy.2016.07.110.
[27] Bo Z, Said MFM, Erdiwansyah E, Mamat R, Xiaoxia J. A review of oxygen generation through renewable hydrogen production. Sustain Chem Clim Action 2025;6:100079. http://dx.doi.org/10.1016/j.scca.2025.100079.
[28] Hirth T. Super – Sustainable production, energy and resources. Chem Ing Tech 2012;84(7). http://dx.doi.org/10.1002/cite.201290061, 943–943.
[29] Toulouevski YN, Zinurov IY. Modern steelmaking in electric arc furnaces: history and development. In: Toulouevski YN, Zinurov IY, editors. Innovation in Electric Arc Furnaces: Scientific Basis for Selection. Berlin, Heidelberg: Springer; 2013, p. 1–24. http://dx.doi.org/10.1007/978-3-642-36273-6_1.
[30] Kleimt B, Dettmer B, Haverkamp V, Deinet T, Tassot P. Erhöhung der energie-und materialeffizienz der stahlerzeugung im lichtbogenofen. 2012, http://dx.doi.org/10.1002/cite.201200076.
[31] Verband der Chemischen Industrie eV(VCI). Produktion anorganischer grundchemikalien in Deutschland 2022 und 2023. Statista 2024.
[32] Kato T, Kubota M, Kobayashi N, Suzuoki Y. Effective utilization of by-product oxygen from electrolysis hydrogen production. Energy 2005;30(14):2580–95. http://dx.doi.org/10.1016/j.energy.2004.07.004.
[33] Elsner H. Edelgase – versorgung wirklich kritisch? – DERA rohstoffinformationen 39:. Technical report, Berlin: Deutsche Rohstoffagentur (DERA); 2018, p. 196.
[34] Verband der Chemischen Industrie eV(VCI). Chemiewirtschaft in Zahlen - 2024. 2024.
[35] Baukal Jr. CE. Oxygen-enhanced combustion. Industrial combustion series, 2nd ed.. Boca Raton: CRC Press, Taylor & Francis Group; 2013, http://dx.doi.org/10.1201/b13974.
[36] Rehfeldt M, Fleiter T, Toro F. A bottom-up estimation of the heating and cooling demand in European industry. Energy Effic 2018;11(5):1057–82. http://dx.doi.org/10.1007/s12053-017-9571-y.
[37] Naegler T, Simon S, Klein M, Gils HC. Quantification of the European industrial heat demand by branch and temperature level. Int J Energy Res 2015;39(15):2019–30. http://dx.doi.org/10.1002/er.3436.
[38] Hörsch J, Hofmann F, Schlachtberger D, Brown T. PyPSA-Eur: An open optimisation model of the European transmission system. Energy Strat Rev 2018;22:207–15. http://dx.doi.org/10.1016/j.esr.2018.08.012.
[39] Brown T, Victoria M, Zeyen E, Hofmann F, Neumann F, Frysztacki M, et al. PyPSA-Eur: An open sector-coupled optimisation model of the European energy system. 2024, http://dx.doi.org/10.5281/ZENODO.11305883, Zenodo.
[40] ORLEN. Agreement for building of the new air separation unit iii in the production plant in Plock. 2022, https://www.orlen.pl/en/investor-relations/reports-and-publications/regulatory-announcements/2022/02/Regulatory-announcement-no-172022.
[41] Agency DE. Technology data for carbon capture, transport and storage. 2024, https://ens.dk/en/our-services/technology-catalogues/technology-data-carbon-capture-transport-and-storage.
[42] lisazeyen, euronion, Neumann F, Millinger M, Parzen M, aalamia, et al. PyPSA/technology-data: V0.9.1. 2024, http://dx.doi.org/10.5281/ZENODO.13255345, Zenodo.
[43] Moore JJ, Pryor O, Cormier I, Fetvedt J. Oxygen storage incorporated into net power and the allam fetvedt oxy-fuel sCO2 power cycle techno-economic analysis. J Eng Gas Turbines Power 2024;146(091021). http://dx.doi.org/10.1115/1.4065048.
[44] Park J, Kang S, Kim S, Kim H, Cho H-S, Lee JH. Comparative techno-economic evaluation of alkaline and proton exchange membrane electrolysis for hydrogen production amidst renewable energy source volatility. Energy Convers Manage 2025;325:119423. http://dx.doi.org/10.1016/j.enconman.2024.119423.
[45] Bundesministerium für Wirtschaft und Klimaschutz. Fortschreibung der Nationalen Wasserstoffstrategie. 2023.
[46] Brown T, Hoersch J, Hofmann F, Neumann F, Victoria M, Zeyen L. Supply and demand — PyPSA-Eur. 2024, https://pypsa-eur.readthedocs.io/en/latest/supply_demand.html.